Facilitation of Human Induced Pluripotent Stem (iPS) Cell Differentiation to Endoderm with a Novel Histone Deacetylase (HDAC) Inhibitor

A DISSERTATION
SUBMITTED TO THE FACULTY OF THE GRADUATE SCHOOL OF THE
UNIVERSITY OF MINNESOTA
BY

Henry O. Aubyn

IN PARTIAL FULFILLMENT OF THE REQUIREMENTS
FOR THE DEGREE OF
MASTER OF SCIENCE

Angela Panoskaltsis-Mortari, PhD, Advisor

June 2016

Acknowledgements

First and foremost, I would like to thank my thesis advisor, Dr. Angela Panoskaltsis-Mortari, for her outstanding guidance and mentoring throughout the course of my research leading to this thesis. My time spent in the lab and with her has helped me grow tremendously, not only as a scientist, but as an individual as well. I also had the pleasure of working with many wonderful individuals in the lab and outside of it. I would specifically like to thank Carolyn Meyer, Andrew Price, Mona Schmidt, Liqiang Chen, Hiroyuki Hirai, Dr. Meri Firpo and Dr. James Dutton. In addition, I would like to thank Dr. Susan Keirstead for her wonderful academic support, mentoring and continuous encouragement. Last, but certainly not least, I would like to thank all the members of the Panoskaltsis-Mortari lab, past and present for all their support and advice as I conducted this research towards my thesis.

Abstract

The use of patient iPS-derived cells for lung regeneration has emerged as a potential tissue engineering strategy for patients with end-stage lung diseases. The ability to efficiently derive lung cells from iPS cells would greatly facilitate the engineering process. Histone deacetylase inhibitors (HDACi) alter gene transcription by inhibiting the deacetylation of lysine residues and have been reported to induce differentiation of cancer stem cells (Botrugno, Santoro, & Minucci, 2009). We are evaluating the ability of a novel HDACi that is an analogue of suberoylanilide hydroxamic acid (SAHA), called SMAHA (Chen, Wilson, Jayaram, & Pankiewicz, 2007), to facilitate differentiation of iPS cells into definitive endoderm. Human iPS cells were generated as previously described (Hirai, Katoku-Kikyo, Karian, Firpo, & Kikyo, 2012). Definitive endoderm differentiation was induced using an established protocol (Mou et al., 2012a) with and without SMAHA at concentrations ranging between 0.0025 and 0.1 μM for 4 days of culture. Gene expression of the pluripotency markers NANOG and OCT-4, and endoderm markers FOXA2 and SOX 17 were assessed by RT-qPCR. The efficacy of SMAHA for inducing iPSCs into definitive endoderm is still under investigation. Preliminary results demonstrated some promise of endoderm induction for iPSCs exposed to SMAHA versus those that were not.

Table of Contents

List of Figures

List of Tables

Introduction

Disease of the lungs and respiratory system in general takes on many forms, from chronic obstructive pulmonary disorder (COPD), which includes emphysema and chronic bronchitis, to cystic fibrosis (CF), obliterative bronchiolitis, and asthma (American Lung Association, 2008). These diseases especially in the young can prove to be fatal and place a heavy burden on families, healthcare and the nation as a whole, in terms of the human and financial resources lost due to such diseases. Lung disease is counted as one of the top three fatal diseases among Americans, being implicated in one out of every six deaths that occur (Miniño, Heron, Murphy, & Kochanek, 2007). Most of these fatalities are seen in the nation's most vulnerable population, infants. In 2004, it was estimated that approximately 20% of infant mortality was due to lung disease and other respiratory impairments (Miniño et al., 2007). Although a number of these diseases may be congenital, a large number are also self-inflicted, the primary form of which is smoking. It is estimated that smoking alone kills one half of a million Americans annually (Centers for Disease Control and Prevention, 2004). The economic cost alone is devastating to a nation, costing hundreds of billions of dollars to the American economy (NIH/NHLBI, 2012).

Embryonic and adult stem cells as well as tissue progenitor cells play roles in organogenesis during embryonic development, adult tissue homeostasis, and in response to internal and external injury. The intrinsic regenerative capacity of the tissue, however, is often limited to overcome the insult. Clinically relevant injuries to the lung include lung cancers, asthma, broncho-pulmonary dysplasia, emphysema, chronic obstructive pulmonary disease, bronchitis, acute respiratory distress syndrome (ARDS), asbestosis, idiopathic pulmonary fibrosis, bronchiectasis, bronchiolitis, byssinosis, cystic fibrosis, hantavirus pulmonary syndrome, histoplasmosis, influenza, and tuberculosis (Ahmad, Shlobin, & Nathan, 2011; R. D. Yusen et al., 2010). Lung transplantation is an effective

treatment where the disease has disabled most of the lung's function. These late stage diseases include cystic fibrosis, COPD, idiopathic pulmonary arterial hypertension, and idiopathic pulmonary fibrosis (Boffini, Ranieri, & Rinaldi, 2010; Roger D Yusen, 2009). Lung transplantations are however limited to the availability of donor lungs, and the immunological complications associated with the graft impairs the success rate. Induced pluripotent stem (iPS) cells can be directed to differentiate into ectodermal, mesenchymal, and endodermal cell types, producing an unlimited quantity of clinically relevant tissue. Endodermal progenitors give rise to organs such as pancreas, liver and lung epithelial cells (Ikonomou & Kotton, 2015). The step-wise differentiation of human iPS cells into lung epithelial cells would help to elucidate the etiologies of human lung disease, facilitate the development of novel treatments, and generate an unlimited source of transplantable tissue. Furthermore, the generation of engineered lung endoderm from patient-derived iPS cells would defeat any immunological complications (Leeman, Fillmore, & Kim, 2014).

The use of patient iPS-derived cells for lung regeneration has emerged as a potential tissue engineering strategy for patients with end-stage lung diseases. The ability to efficiently derive lung cells from iPS cells would greatly facilitate the engineering process. Induced pluripotent stem cells are derived from fetal or adult cells through reprogramming using four key transcription factors, namely Oct4, Sox2, c-Myc, and Klf4.[7] These iPS cells possess identical characteristics with embryonic stem (ES) cells, such as expression of pluripotency markers, ES cell morphology, self-renewal, and the capability of teratoma formation (Takahashi et al., 2007).

The foregut endoderm gives rise to the lung epithelium. Genetic programs cause the formation of the gut tube, liver, pancreas and ultimately the formation of the trachea and lung (Wong & Rossant, 2013). As the lung matures, cells differentiate into their terminal stage and replication decreases. Studies have shown that the adult lung

possesses some regenerative potential, but its reach is very limited (Evans, Cabral, Stephens, & Freeman, 1973; Peake, Reynolds, Stripp, Stephens, & Pinkerton, 2000; Van Winkle, Buckpitt, Nishio, Isaac, & Plopper, 1995). Attempts to induce self-repair by activating dormant lung stem cells have shown some success (Wong et al., 2009). However, studies taking a step-wise approach of differentiating embryonic stem cells or iPS cells by mimicking the different stages of normal lung morphogenesis have been more promising. Human and mouse ES cells were differentiated into ventral foregut endoderm (Green et al., 2011; Longmire et al., 2012); also, human and mouse iPS cells were differentiated into multipotent lung and airway progenitors (Mou et al., 2012b; Schmeckebier et al., 2013). Although promising, these approaches are limited and further improvement is needed.

Chromatin modifications, such as DNA methylation and histone deacetylation comprise major complex biochemical and cellular mechanisms. The modifications play a role in epigenetic regulation of gene expression during development and differentiation, and are also involved in nucleosome assembly and chromatin folding (Cedar & Bergman, 2009; B. Li, Carey, & Workman, 2007; E. Li, 2002). The modern mammalian genome comprises eighteen genes coding for histone deacetylases. They are grouped into four families. Class I (comprising HDACs 1, 2, 3 and 8); IIa (HDACs 4, 5, 7 and 9); IIb (HDACs 6 and 10); III (SIRTUINs 1–7); and IV (HDAC 11) (X.-J. Yang & Seto, 2008). HDACs 1 and 2 perform roles in the differentiation of neuronal precursors into neurons (Montgomery, Hsieh, Barbosa, Richardson, & Olson, 2009); and in hematopoiesis (Wilting et al., 2010). HDAC1 activity plays a role in erythroid differentiation, where it blocks myeloid differentiation (Wada et al., 2009). Conditional tissue-specific deletions of HDAC3 revealed an involvement in liver (Knutson et al., 2008), and heart (Montgomery et al., 2008) function. Class I HDACs are widely expressed, but members of the class IIa show tissue- restricted expression. HDAC4 regulates skeletogenesis

(Vega et al., 2004). HDACs 5 and 9 control skeletal muscle differentiation and HDAC7 is expressed in endothelial cells of the cardiovascular system (Chang et al., 2006; M.-S. Kim et al., 2008; Méjat et al., 2005). Histone deacetylation can be inhibited *in vitro* and *in vivo* eliciting pleiotropic effects on cell homeostasis. Histone deacetylase inhibitors (HDACi) comprise natural or synthetic small molecules, and are grouped into four classes according to structure, these include: cyclic peptides, benzamides, hydroxamates and aliphatic acids (H.-J. Kim & Bae, 2011). Under developmental conditions, such HDACi can promote self- renewal or differentiation of stem cells, such as embryonic stem cells, iPS cells or adult stem cells. In addition, HDACi may enable direct differentiation of embryonic and tissue-specific stem cells along the neuronal, cardiomyocytic, or hepatic lineages (Kretsovali, Hadjimichael, & Charmpilas, 2012). Inhibitors of class I and II HDACs fall into structural categories including hydroxamic acids (e.g., trichostatin A), cyclic peptides (including cyclic tetrapeptides (such as trapoxin B and depsipeptides)), electrophilic ketones, aliphatic acid compounds (including phenylbutyrate and valproic acid), benzamides, benzofuranone, and sulfonamide containing molecules (Marks & Breslow, 2007; Yoshida, Matsuyama, Komatsu, & Nishino, 2003). Additional examples of such inhibitors include, but are not limited to, the hydroxamic acids belinostat (PXD101), LAQ824, vorinostat (SAHA), and panobinostat (LBH589); and the benzamides: entinostat (MS-275), CI994, and mocetinostat (MGCD0103); and nicotinamide (NAD), as well as derivatives of NAD, dihydrocoumarin, naphthopyranone, and 2-hydroxynaphaldehydes. The biological effects of HDACi result from positive or negative regulation of gene expression by the controlled acetylation of histones, transcription factors, or other proteins (Marks & Breslow, 2007; Yoshida et al., 2003). One class of HDACi consists of hydroxamic acid compounds. Suberoylanilide hydroxamic acid (SAHA; *N*-hydroxy-*N*'-phenyl-octanediamide) is a member of the hydroxamic acid class of the newly developed histone

deacetylase inhibitors. SAHA's function has been implicated in anti-tumor activity: SAHA was reported to inhibit the growth of paclitaxel-resistant ovarian cancer OC3/P cells (Liu et al., 2014); SAHA has also been approved for the treatment of a form of skin cancer known as cutaneous T cell lymphoma (CTCL) and acts against B cell lymphoma A20 cells *in vitro* and *in vivo* (B. Yang et al., 2015). Modification of SAHA with chemical groups designed to interact with HDACs led to the synthesis of the SAHA analogue 14, henceforth, known as SMAHA (Chen et al., 2007; Lai et al., 2012).

The positive charge associated with histones and the negatively charged DNA-phosphate backbone leads to a mutual attraction between the two entities. The attraction results in the DNA being tightly wound around the histones and hence inhibiting transcription to a degree. Histone acetyltransferases (HATs) add acetyl groups to lysine residues on histone tails, thereby decreasing the positive charge on the histones and making them more neutral. This eventually decreases the attraction between the histones and the DNA, leading to separation and allowing transcription to take place. This process can however be reversed by the removal of such acetyl groups by histone deacetylases (HDACs). HDACi such as SMAHA prevent this from happening and in turn allow the chromatin to remain open longer allowing various cellular processes to continue, such as differentiation. HDACs 1 and 2 have been implicated in the suppression of tumor suppressors such as retinoblastoma 1 (Rb1), p16 and p21 hence allowing proliferation of endoderm progenitors during development, and also allowing regeneration of the airways to take place (Herriges & Morrisey, 2014; Wang et al., 2013). A balance must be struck between the HATs and HDAC activity if the endoderm differentiation is to take place properly and allow proper development of the lungs (Herriges & Morrisey, 2014). Many epigenetic mechanisms are involved in the differentiation process. There are genes that are upregulated and some downregulated during the differentiation process even though they are involved in the same epigenetic mechanism. Aside from the effects that

SMAHA and the differentiation process as a whole may have on HATs and HDACs, other epigenetic mechanisms affected, that is either being upregulated or downregulated include: DNA and Histone Methyltransferases, SET Domain Proteins (Histone Methyltransferase Activity), Histone Phosphorylation, Histone Ubiquitination, and; DNA and Histone Demethylases. SMAHA may also affect non-histone proteins such as signaling molecules, transcription factors and chaperones (H.-J. Kim & Bae, 2011). This may in turn impact other processes such as protein-DNA and protein-protein interactions in addition to protein stability (Glozak, Sengupta, Zhang, & Seto, 2005; H.-J. Kim & Bae, 2011).

Endoderm differentiation from iPS cells is currently inefficient and variable from laboratory to laboratory. The aim of this project is to determine whether the HDACi SMAHA can facilitate the differentiation of iPS cells into endoderm, with a greater efficiency. Such cells could find use in, for example, lung and pancreatic clinical and pre-clinical applications. Here a method is provided to differentiate iPS cells into cells of an endodermal lineage which involves treating the iPS cells with a number of endoderm differentiation factors with and without SMAHA. This differentiation is carried out *in vitro*. The endodermal lineage cell comprises increased FOXA2 and/or SOX17 expression, and decreased NANOG and/or OCT4 expression as compared to the parent (undifferentiated) iPS cells. The endoderm differentiation factor consists of a basal media with Activin A (a TFGβ agonist), a PI3K inhibitor (LY294002) and/or the HDACi SMAHA (SMAHA is an analogue of suberoylanilide hydroxamic acid and is a modified compound of the parental chemical *N*-hydroxy-*N*'- phenyl-octanediamide, also known as SAHA). The concentration of SMAHA is between 0.0025 and 0.1 μM. The efficacy of SMAHA for inducing iPSCs to definitive endoderm is still under investigation. Preliminary results demonstrated some promise of endoderm induction for iPSCs exposed to SMAHA versus those that were not.

Materials and Methods

Cell Lines Used

Hiro Cell Line

Human induced pluripotent stem (iPS) cells were generated from bone marrow by transducing a fusion gene composed of OCT4, SOX2, KLF-4 and c-Myc, and the transactivation domain of MyoD, after which the transduced cells were cultured at a low density in serum-free culture conditions (Hirai, Firpo, & Kikyo, 2012; Hirai, Katoku-Kikyo, et al., 2012).

vShiPS 9-1 Cell Line

An additional cell line used called vShiPS 9-1was a gift from Dr. James Dutton. The vShiPS 9-1 induced pluripotent stem cell line was generated by reprogramming neonatal dermal fibroblasts with CytoTune® 1.0 Sendai Reprogramming vectors (Ye et al., 2013). The iPSCs were derived on irradiated mouse embryonic fibroblasts in human embryonic stem cell media containing Knockout serum replacer. Characterized vShiPS 9-1 cells were subsequently adapted for culture in Essential 8 media on recombinant Vitronectin. The vShiPS 9-1 cells have been extensively characterized by the Progenitor Cell Biology Consortium Research of the National Heart, Lung, and Blood Institute (NHLBI/PCBC) Cell Characterization Core facility.

L1 Cell Line

Derivation of L1 iPS cell lines: The day before lentiviral transduction, 1.25 x 10^5 Normal Human Dermal Fibroblast (NHDF) (Lonza, Basel, Switzerland) cells were seeded on a gelatin coated 6-well plate in growth medium containing high-glucose DMEM, 10% FBS, and 0.1mM non-essential amino acids (NEAA). A mixture of 4 different recombinant lentiviruses expressing human Oct4, Sox2, Nanog, and Lin28 were used to infect the NHDF cells in the presence of 8 μg/ml polybrene (Sigma-Aldrich, St. Louis, MO). After overnight incubation with the mixture, the medium containing viruses was replaced with fresh growth medium. Four days after transduction, 5.5 x 10^4 cells

were collected by trypsin (Invitrogen, Carlsbad, CA) digestion and transferred onto irradiated mouse embryonic fibroblast (MEF) cells in each well of a 6-well plate containing human embryonic stem (hES) cell medium: DMEM/F12 medium containing 20% knockout serum replacement, 0.1mM NEAA, 1mM L-glutamine, 0.1mM β-mercaptoethanol and 4 ng/ml basic fibroblast growth factor (bFGF). IPS colonies with typical hES cell morphology appeared 15 days post-transduction and were picked for expansion on day 26.

Lentivirus production: Each recombinant lentivirus expressing human Oct4, Sox2, Nanog, and Lin28 was generated by transfecting the constructors (Addgene 16579, 16577, 16578, 16580) together with packaging plasmid pΔNRF and MDG into 293FT cells. Briefly, 4.5 x 10^6 293FT cells were seeded using DMEM medium supplemented with 10% FBS in 15 cm plates. The transfection was conducted the next day using a calcium-phosphate-mediated method. Twenty hours after transfection, the medium was changed to DMEM with 2% FBS. Viral supernatants were harvested at 24 and 48 hours post-transfection and concentrated by ultracentrifugation at 22,000 rpm for 2 hours.

Maintenance of hiPSC Lines

The hiPSCs were grown in E8 media on Synthemax-coated plates. The cells were fed every day and passaged at 65-80% confluence (~ every 3-4 days) at a ratio of 1:6. On the day before splitting, the Synthemax was aliquoted, and the appropriate number of plates coated for the next day. To split the iPSCs, the media was aspirated and the cells washed with PBS. The PBS was then aspirated and the EDTA solution applied (1 ml per 6-well plate). The cells were incubated at room temperature and the colonies observed under a microscope. When the cells began to lose shape and detach, the dish was agitated to facilitate the detachment. PBS was then added and pipetted up and down several times gently to dissociate the cells from the dish and also make a single-cell suspension. The cell suspension was then transferred into a 50 ml falcon tube and spun at 1000 RPM for 5 minutes. The supernatant was then aspirated and the cells resuspended in an appropriate volume of E8 media. The Synthemax coating solution was then aspirated from the new

Synthemax-coated plates, and the cell solution transferred to the freshly-coated plates. The cells were maintained in an undifferentiated state in a 5% CO_2 environment.

Induction of Definitive Endoderm

Two days prior to endoderm differentiation the human iPS cells were seeded at 35-40% confluency. Cells of such confluent cultures were allowed to grow for two days in Essential 8 (E8) media (Life Technologies Corp, Carlsbad, CA). On the day the differentiation experiments were to commence, the E8 media was aspirated, and the wells rinsed twice with warm RPMI-1640 (GIBCO, Carlsbad, CA) to remove residual growth factors. Each well received 3mL of endoderm differentiation media containing 2% B27 without retinoic acid (GIBCO), 0.1% Albumax II (GIBCO), 1% Glutamax (GIBCO), 1% 1X non-essential amino acids (GIBCO), 1% Penicillin/streptomycin, Activin A (100ng/mL, R&D Systems) and PI3K inhibitor (5uM, Tocris Bioscience) (Mou et al., 2012a) (Figure 1). One-tenth of a milligram of SMAHA (Liqiang Chen, Center for Drug Design, University of Minnesota) was dissolved in 1mL of 100% DMSO (Sigma-Aldrich, St. Louis, MO) to obtain a stock concentration of 276.88µM. Serial dilutions were performed by adding 200µL of the stock solution to 800µL of RPMI media to obtain a concentration of 55.4µM. All culture conditions were set up in duplicate for each experiment. To obtain a concentration of 0.05µM SMAHA, 5.4µL of the first serial dilution was added to 6mL of endoderm differentiation media. For 0.1µM SMAHA concentration, 10.8µL of the first serial dilution was added to 6mL of endoderm differentiation media. The media was changed daily and the cells were differentiated for four days.

Induction of Anterior Foregut Endoderm

On the fourth day, the definitive endoderm cells were rinsed with warm RPMI twice to remove residual factors. The cells were then directly treated with anteriorization buffer which consisted of: RPMI-1640 (GIBCO, Carlsbad, CA), 2% B27 without retinoic acid (GIBCO), 0.1% Albumax II (GIBCO), 1% Glutamax (GIBCO), 1% 1X non-essential amino acids (GIBCO), 1% Penicillin/streptomycin, 1.5 µM TGFβ antagonist A-8301

(CalBiochem) and 300 nM WNT antagonist IWR-1 (Tocris Bioscience). A separate media was also made that contained the same ingredients in addition to 0.1µM SMAHA, and used to culture cells. In both cases the media was changed daily and the cells were differentiated for four days.

Induction of Lung Endoderm (NKX2.1+) Cells

Once the anteriorization step was complete, the cells were washed with PBS and the NKX2.1 induction media added. The NKX2.1 induction media consisted of: RPMI-1640 (GIBCO, Carlsbad, CA), 2% B27 with retinoic acid (GIBCO), 0.1% Albumax II (GIBCO), 1% Glutamax (GIBCO), 1% 1X non-essential amino acids (GIBCO), 1% Penicillin/streptomycin, 10 ng/ml BMP4 (Stemgent), 100ng/mL FGF2 (Tocris Bioscience) and 25 nM GSK3iXV, a WNT agonist (Tocris Bioscience). A separate media was also made that contained the same ingredients in addition to 0.1µM SMAHA, and used to culture cells. In both cases the media was changed daily and the cells were differentiated for four days.

Immunofluorescence

Cells were fixed with fresh 4% paraformaldehyde for 15 minutes at room temperature, rinsed to remove any residue, then washed with a solution of PBS and 0.2% Triton X-100, followed by incubation with primary antibodies overnight at 4^{o}C. The primary antibodies were diluted in PBS containing 0.3% bovine serum albumin (BSA). After the incubation period, the cells were washed several times with PBS containing 0.2% Triton X-100 and incubated with secondary antibodies for 30 minutes at room temperature. The images were visualized using an Olympus BX51 epifluorescence microscope. The primary antibodies used are listed in Table 1.

Real Time Quantitative Polymerase Chain Reaction (RT-qPCR)

RNA was isolated using both Trizol Reagent (Invitrogen) and RNeasy kit (Qiagen, Valencia, CA) following the manufacturer's protocol. Both the RNA concentration and quality were measured with an Implen NanoPhotometer P330. 2-5 µg of total RNA was

reverse transcribed to cDNA using SuperScript III Reverse Transcriptase (Invitrogen) with random hexamers (Life Technologies) following the manufactures instructions. Up to 8 µL of cDNA was used in a 25 µL real time PCR reaction using TaqMan Gene Expression Master Mix (Applied Biosystems) and an ABI 7500 Real Time PCR System. The real time PCR conditions were 95^{o}C for 10 minutes followed by 40 cycles of 95^{o}C for 15 seconds and 60^{o}C for 1 minute. For each gene, the absolute quantification was obtained and normalized to the housekeeping gene, GAPDH. Quantitative PCR for each sample was performed at least in triplicate. For gene expression analyses, the following probes (Applied Biosystems, Foster City, CA) were used: NANOG: Hs02387400_g1, SOX17: Hs00751752_s1, GAPDH: 02758991_g1, OCT4: 04260367_gH and FOXA2: Hs00232764_m1, CDH5: Hs00901463_m1, GATA4: Hs00171403_m1, FOXA1: Hs04187555_m1, EPCAM: Hs00901885_m1, C-KIT: Hs00174029_m1, GATA6: Hs00232018_m1, NCAM1: Hs00941830_m1, CDX2: Hs01078080_m1, CXCR4: Hs00607978_s1, SOX2: Hs01053049_s1, CD34: Hs00990732_m1 and NKX2.1: Hs00968940_m1.

Flow Cytometry

After the appropriate differentiation period, the media was aspirated and the cells were washed with PBS to remove any residual factors. A single cell suspension was obtained with the aid of EDTA. The cells were then washed with FACS (Fluorescence Activated Cell Sorting) buffer, which was a solution of PBS and 0.3% BSA, centrifuged at 300 x g for 5 minutes and then decanted to obtain a pellet of cells. For intracellular markers, the cells were fixed with 4% paraformaldehyde and incubated at room temperature for 10 minutes. The cells were then washed again with the FACS buffer and centrifuged at 300 x g for 5 minutes and then decanted to obtain a pellet of cells. 100 µl of 0.2% Triton X-100 was then added to the cells and incubated at room temperature for 15 minutes. Afterward, for both the cell surface and intracellular markers, the primary antibody was added to the cells, and incubated in the dark for one hour. The cells were then washed with the FACS buffer, centrifuged at 300 x g for 5 minutes and then decanted, after which the cells were resuspended in FACS buffer and the single cell suspension strained

before proceeding to flow cytometric analysis. Cells were also briefly vortexed intermittently to maintain a single cell suspension. The cells were directly stained with FITC-conjugated FOXA2 and APC-conjugated SOX17, or PE-conjugated CXCR4 and Brilliant Violet (BV) 650-conjugated C-KIT. All primary antibodies used were obtained from Invitrogen. Stained cells were analyzed using a LSRII (BD Biosciences) at the University of Minnesota's core facility and the results obtained were analyzed by Flowjo software (Tree Star, Ashland, OR).

Statistical Analysis

Statistical analysis was conducted using one-way analysis of variance (ANOVA) followed by Tukey's multiple comparisons test, with a single pooled variance. Results were shown as Mean ± SEM, where p-Values <0.05 were considered statistically significant.

Results

Differentiation of Human Induced Pluripotent Stem Cells into Definitive Endoderm with the L1 Cell Line

The stepwise differentiation of iPSCs into lung endoderm has been outlined in Figure 1. The induction of definitive endoderm from iPSCs was achieved by culturing the iPSCs in definitive endoderm differentiation media for four days, with a daily media change as described in the methods. The differentiation into definitive endoderm was performed on three different cell lines namely the L1, Hiro and vShiPS cell line. Of the several different conditions tested in the L1 cell line, only one condition exhibited a very significant difference in the fold increase expression of FOXA2 via RT-qPCR, this was the condition consisting of Activin and the phosphoinositide 3-kinase inhibitor (PI3Ki) as expected (Figure 2A). All other conditions examined showed varying degrees of FOXA2 expression but none were comparable to the Act + PI3Ki condition, when they were compared to the negative control which comprised undifferentiated iPSCs (Figure 2A). When SOX17 expression was examined via RT-qPCR, a very high fold increase was observed in the condition that received the Activin + PI3Ki when compared to the undifferentiated iPSCs, just as in the FOXA2 expression (Figure 2B). In addition to this, a significant difference was observed between the conditions that received 0.05uM drug + Activin + PI3Ki, and 0.1uM drug + Activin when compared to the undifferentiated iPS cells (NC = negative control) (Figure 2B), although none of these conditions were comparable to the Act + PI3Ki condition. Throughout the differentiation process, the pluripotency marker OCT4 decreased significantly in expression for two conditions when compared to the undifferentiated iPS cells: 0.05uM drug only, and 0.1uM drug only (Figure 2C). A few conditions led to varying increases in the expression of OCT4 after four days of differentiation (Figure 2C). The other pluripotency marker examined was NANOG in which there was a very significant decrease in two conditions. These decreases in NANOG expression was observed in cells that received media containing 0.05uM drug only or 0.1uM drug only (Figure 2D). Next, genes involved in the mesodermal lineage were examined to determine the effect that this definitive endoderm

differentiation protocol in the presence or absence of SMAHA (simply referred to as "drug" in some cases) has on the expression of genes that are involved in the mesodermal lineage. The subsequent genes examined did not have as many conditions as that of OCT4, NANOG, FOXA2 and SOX17 because by the time it was decided to assess these genes, previous optimization experiments had determined that the SMAHA concentration of 0.1uM was best. Of the conditions tested in the expression of CD34, only the Act + PI3Ki condition showed a significant difference with an approximately 5-fold decrease in expression levels (Figure 2E). CDH5 was another gene corresponding to the mesodermal lineage for which its expression due to the various conditions used was examined. Here there seemed to be a significant difference in the 0.1uM drug + Act + PI3Ki condition with respect to the negative control, with an approximate 7-fold increase in gene expression (Figure 2F). The NCAM1 gene was examined to determine how the conditions used affect the expression of this gene that is expressed in cells that constitute the ectodermal lineage. NCAM1 expression was increased 8-fold in cells that were exposed to differentiation media that also contained 0.1uM drug, in addition to the Activin and PI3Ki (Figure 2G). The expression of several other endodermal genes was examined to determine how the various conditions used affect the expression of these genes. These genes included: EPCAM, FOXA1, GATA4, GATA6, CXCR4 and C-KIT. For the purposes of this experiment, C-KIT was deemed as an endodermal marker (Mou et al., 2012b). Others have labeled C-KIT as an indicator of stem cells (Bearzi et al., 2007; Beltrami et al., 2003; Kajstura et al., 2014; Orlic, Fischer, Nishikawa, Nienhuis, & Bodine, 1993). C-KIT expression was elevated with a significant difference in one condition, namely Activin + PI3Ki with a fold increase of 2.4 when compared to the undifferentiated iPS cells (Figure 2H). The condition of 0.1uM drug + Activin + PI3Ki was shown to exhibit no significant difference (Figure 2H). CXCR4 was shown to have an increased expression in the presence of all three conditions (Figure 2I). For EPCAM, only the AHL showed a significant increase in gene expression when compared to the undifferentiated iPS cells (Figure 2J). FOXA1 showed elevated gene expression in one condition which was the Activin + PI3Ki with a fold increase of approximately 125 (Figure 2K). GATA4 analysis revealed increased gene expression in the Activin + PI3Ki,

and the 0.1uM drug + Activin + PI3Ki condition, with a fold increase of approximately 274 and 35 respectively, when compared to the undifferentiated iPS cells (Figure 2L). In the analysis of GATA6, two conditions compared to the undifferentiated iPS cells revealed a significant increase in gene expression with fold increases of approximately 170 and 146 for the conditions of 0.1uM drug + Activin + PI3Ki, and Activin + PI3Ki, respectively (Figure 2M).

Undifferentiated L1 cells expressed both pluripotency transcription factors OCT4 and NANOG; the undifferentiated cells however did not coexpress both pluripotent transcription factors, OCT4 was however expressed predominantly (Figure 3A). As expected, both endoderm makers, FOXA2 and SOX17 were not expressed (Figures 3B and C). Similar results were obtained via flow cytometry where 99.5% of undifferentiated cells were negative for the coexpression of FOXA2 and SOX17 (Figure 3D). Differentiated L1 cells (in the presence of SMAHA) expressed very low levels of FOXA2 (Figure 3E). L1 cells differentiated in the absence of SMAHA had few cells expressing FOXA2 as well (Figure 3F). SOX17 expression among L1 cells that were differentiated in the presence of SMAHA was undetectable (Figure 3G). L1 cells differentiated in the absence of SMAHA had no cells expressing SOX17 that was detectable (Figure 3H), similar to those L1 cells cultured in the presence of drug. The pluripotent transcription factor NANOG remained undetectable in those cells that were cultured with SMAHA (Figure 3I). The pluripotent transcription factor NANOG also remained undetectable (Figure 3J) in cells cultured in the absence of SMAHA. OCT4 was detectable in cells that were cultured with SMAHA (Figure 3K). The pluripotent transcription factor OCT4 was easily detected in cells cultured in the absence of SMAHA as well (Figure 3L). When L1 cells differentiated in the presence of SMAHA were analyzed via flow cytometry, only 10% of cells coexpressed FOXA2 and SOX17 (Figure 3M). In cells differentiated in the absence of SMAHA, 36% of cells coexpressed FOXA2 and SOX17 when analyzed via flow cytometry (Figure 3N). For the L1 cell line, cell morphology varied between a few of the different culture conditions. A decrease in cell quantity was observed when cells were cultured in the presence of SMAHA (Figure 4),

with an average cell viability of approximately 80% compared to approximately 90% for cells not treated with SMAHA. From the above data with the L1 cell line, it appears that SMAHA does not facilitate increased expression of endodermal genes. SMAHA led to a decrease in the expression of the pluripotency genes examined but there was not a corresponding increase in the endodermal genes FOXA2 and SOX17. SMAHA however led to increased gene expression in both mesodermal and ectodermal genes.

Differentiation of Human Induced Pluripotent Stem Cells into Definitive Endoderm with the Hiro Cell Line

The same set of RT-qPCR evaluations of gene expression performed on the L1 cell line was performed on the Hiro cell line as well. Several conditions led to a significant increase in the expression of FOXA2 when compared to the undifferentiated iPS cells including: 0.005uM drug only (6.5-fold), 0.05uM drug + Activin (21.5-fold), 0.05uM drug + Activin + PI3Ki (31-fold), 0.1uM drug + Activin (27-fold), 0.1uM drug + Activin + PI3Ki (14.5-fold), Activin + PI3Ki (5-fold), and Activin + PI3Ki + DMSO (211-fold) (Figure 5A). A number of culture conditions also led to significant increases in the expression of SOX17, including 0.05uM drug + Activin + PI3Ki (41-fold), 0.1uM drug + Activin (49-fold), 0.1uM drug + Activin + PI3Ki (250-fold), Activin + PI3Ki (143-fold), and Activin + PI3Ki + DMSO (436-fold) (Figure 5B). Upon assessing the expression levels of OCT4 when exposed to various culture conditions, there was a significant decrease in gene expression only in the AHL (≈ 30-fold decrease), which would be expected since the AHL cells were terminally differentiated and hence expressed very little pluripotency (Figure 5C). NANOG, the other pluripotency marker examined did not lead to any significant changes in any of the cells that received any of the various combinations of conditions, with the exception of the AHL (Figure 5D). CD34 and CDH5, both used to determine if some of the cells were being guided towards the mesodermal lineage showed significant increases only in the AHL with fold increases of approximately 2,175 and 140,576, respectively (Figures 5E and 5F). Considering the

high cycle threshold (≈ 35) that was associated with the CDH5 fold increase, it is more likely that there was little to no actual increase in CDH5 gene expression. It was observed that NCAM1expression levels, used to determine if some cells were being guided towards the ectoderm lineage, were significantly elevated in both the AHL (8-fold) and 0.1uM drug + Activin + PI3Ki (≈ 4-fold) (Figure 5G). Once again several other endodermal genes were analyzed to determine the effects the various conditions used had on the expression of these genes. The genes included: CXCR4, EPCAM, FOXA1, GATA4, GATA6, and for the specific purpose of this study, C-KIT. CXCR4 expression levels were significantly elevated in all four conditions used when compared to the undifferentiated iPS cells (Figure 5H). Although C-KIT, EPCAM and FOXA1 showed varying degrees of expression increase, the increases however, occurred in the same conditions: Activin + PI3Ki, Activin + PI3Ki + DMSO, and AHL (Figures 5I, 5J and 5K). GATA4 expression levels were significantly elevated in all but one of the conditions tested whereas GATA6 expression was significantly elevated in all four conditions (Figures 5L and 5M). A few of the conditions tested led to a small number of cells expressing significant levels of NKX2.1, the earliest marker for lung endoderm. This gene however is usually expressed in cells that are further along the differentiation process as opposed to the initial stages. These three conditions however, expressed significantly elevated levels of the NKX2.1 gene: 0.0025uM drug + Activin + PI3Ki, Activin + PI3Ki, and Activin only (Figure 5N).

Undifferentiated Hiro cells were stained with various antibodies to determine the expression levels of key genes. The undifferentiated cells expressed the pluripotent transcription factors OCT4 and NANOG, although NANOG seemed to be expressed very weakly. The cells did not seem to coexpress NANOG and OCT4; instead OCT4 was primarily expressed in the Hiro cell line (Figure 6A). The endodermal genes, FOXA2 and SOX17 were also stained for to determine if any spontaneous differentiation had taken place. Both FOXA2 and SOX17 expression was not detected which was expected since the cells were undifferentiated and remained in the pluripotent state (Figures 6B and 6C). Similar analyses were performed on undifferentiated cells using flow cytometry.

Approximately 93% of undifferentiated cells were negative for FOXA2 and SOX17 coexpression (Figure 6D). Hiro cells that were differentiated in the presence of SMAHA were also examined for both pluripotency and differentiation markers. FOXA2 expression was very minimal with few cells expressing the transcription factor (Figure 6E). Given the relatively high expression levels that were observed via RT-qPCR, this may indicate that a very few number of cells were expressing high levels of the FOXA2 transcription factor as opposed to numerous cells expressing modest levels of FOXA2. The expression levels of FOXA2 in cells that were differentiated in the absence of SMAHA were similar to those that were differentiated in the presence of SMAHA. A few cells showed expression of FOXA2 (Figure 6F), and this may be due to the same reasoning that was stated earlier. For cells cultured in the presence of SMAHA, SOX17 seemed to be expressed at modest levels among numerous cells (Figure 6G). For cells cultured in the absence of SMAHA, SOX17 was not detected (Figure 6H). There was no expression of the pluripotency marker NANOG among the cells cultured with SMAHA (Figure 6I). NANOG was not detected in cells cultured in the absence of SMAHA (Figure 6J) as well. Expression of OCT4 among cells cultured in the presence of SMAHA was easily detected (Figure 6K). This was not surprising considering that in the early stages of the differentiation process, it was expected that some of the cells would remain in the pluripotent state. OCT4 was detected in cells cultured in the absence of SMAHA as well (Figure 6L). Flow cytometric analysis also revealed that 46% of cells cultured in the presence of SMAHA coexpressed FOXA2 and SOX17 (Figure 6M). Flow cytometric analysis also revealed that approximately 15% of cells cultured in the absence of SMAHA coexpressed FOXA2 and SOX17 (Figure 6N). Also, the morphology of Hiro cells did not seem to vary for the most part with the different culture conditions (Figure 7), and in terms of the cell viability, the average viability of cells treated with SMAHA was approximately 89% compared to approximately 87% for cells not treated with SMAHA. This demonstrates that SMAHA was neither toxic to the cells, nor did it decease cell viability when compared to cells not treated with SMAHA. SMAHA led to neither an increase nor a decrease in the expression of the pluripotency genes OCT4 or NANOG. Overall, increased gene expression was however observed in genes from all

three germ layers. Upon further examination, it can be seen that the Act + PI3Ki + DMSO condition led to very significant increases in genes of the endodermal lineage, however even though conditions such as 0.1uM drug + Act + PI3Ki led to increases in endodermal genes, they were not as high. This may mean that DMSO by itself may be facilitating differentiation into the endodermal lineage and that the drug, which is dissolved in DMSO may actually be inhibiting differentiation into endoderm.

Differentiation of Human Induced Pluripotent Stem Cells into Lung Endoderm with the vShiPS Cell Line

The final cell line examined via RT-qPCR was the vShiPS. With these cells, various drug concentrations were not used because by this time, it was determined that the drug concentration of 0.1uM drug (SMAHA), was the optimal choice. With the vShiPS cell line, the differentiation process was carried on beyond the definitive endoderm stage, which was not the case in the other two cell lines tested, which is the L1 and the Hiro cell line. The vShiPS were differentiated for two additional stages, including the anteriorization of the definitive endoderm into foregut endoderm (AFE), followed by the generation of NKX2.1+ lung endoderm from the anterior foregut cells (LE). With each step of the differentiation performed according to the established protocol (Mou et al., 2012b), a corresponding setup was done which was identical to the former with the exception that SMAHA was added to the differentiation protocol, which is commonly referred to as "drug". Another differentiation setup was performed with a few modifications to the established protocol (Mou et al., 2012b). In this setup, the induction of definitive endoderm from human iPSCs was performed according to protocol, but afterwards, the cells were FACS sorted for $CXCR4^{+}$ definitive endoderm cells. Undifferentiated cells predominantly expressed C-KIT (Figure 8A), while after four days of definitive endoderm differentiation, the cells predominantly expressed CXCR4 (Figure 8B), and were sorted for and the subsequent differentiation steps continued. Sixty-six percent of these sorted cells coexpressed FOXA2 and SOX17 (Figure 8C). The

subsequent differentiation processes were conducted according to protocol with each setup having its corresponding setup that included the addition of 0.1uM SMAHA. These cells were differentiated into lung endoderm after which the expression levels of various genes were analyzed via RT-qPCR, as in the other two cell lines. The expression levels of the various genes analyzed throughout the various stages are shown in figures 9A-9O. The vShiPS cell line was the only cell line in which the cells were differentiated beyond the definitive endoderm stage. Definitive endoderm induction was conducted in the absence of SMAHA, but all subsequent conditions and differentiations were done in either the presence or absence of SMAHA. Cell morphology did vary somewhat between different differentiation stages (Figure 10). With respect to cell viability, the average viability of cells differentiated into definitive endoderm was approximately 90%. Approximately 85% of cells treated with SMAHA and differentiated into anterior foregut endoderm were viable, compared to 80% of such cells that were not treated with SMAHA. SMAHA induced lung endoderm was 70% viable while those that were not SMAHA induced were 75% viable. CXCR4+ definitive endoderm sorted cells that were further differentiated into lung endoderm in the presence of SMAHA had a cell viability of 90%, while those same cells without SMAHA were approximately 60% viable. Overall, for the vShiPS cell line, there seems to be a decrease in the expression of the various genes examined when cells are cultured in the presence of SMAHA. Just as in the other cell lines, the conclusion can be made that the drug does not seem to facilitate the differentiation of the iPS cells towards the endodermal lineage.

Discussion

This study investigates the efficacy of SMAHA in its ability to facilitate the induction of iPSCs into definitive endoderm, which can subsequently be differentiated into anterior foregut endoderm, and then into NKX2.1+ lung endoderm. The achievement of this can further lead to the differentiation of a number of cell types of the respiratory system. Such cells can then be seeded onto a decellularized lung scaffold in the hopes of bioengineering a lung for transplantation. Significant expression levels of the definitive endoderm genes FOXA2 and SOX17 were observed, and these results were comparable to those of the study from which this project was based. In addition, significant expression levels of genes indicative of the mesodermal and ectodermal lineages such as CDH5, CD34 and; NCAM1 respectively, were observed. Table 2 summarizes the varying gene expression among the three cell lines used. The expression of such genes may be useful as they are needed for the proper function of the respiratory system as a whole, since such genes lead to the development of structures such as cartilage, smooth muscle and nerves. Despite the meticulous optimization performed, it did not prove to be enough due to low NKX2.1 expression levels within the lung endoderm cells generated. The concentration of various factors may need to be modified for each cell line used, in addition to when the appropriate factors are added. New concentrations may even need to be experimented with to achieve the desired results. The WNT agonist GSK3 is one factor needed to differentiate the anterior foregut endoderm into lung endoderm, but when added prematurely, or at too high of a concentration, it can drive the cells past lung endoderm and rather towards the hindgut fate (Cao et al., 2011; Mou et al., 2012b; Sherwood, Maehr, Mazzoni, & Melton, 2011; Spence et al., 2010). The low number and expression of both NKX2.1+ cells and cells coexpressing FOXA2 and SOX17 may be due to a number of factors such as the interaction of multiple pathways that affect NKX2.1+ cell induction in one way or another, or the fact that a number of other pathways may need to be activated, or inhibited at certain time points to achieve the desired results, such as the WNT signaling pathway. Another consideration to take into account is the fact that in vitro experiments may not always recapitulate what transpires

in vivo. In vivo experiments can be performed where FOXA2+/SOX17+ definitive endoderm can be placed under the kidney capsule of an immune deficient mouse. This may serve as a baseline to assess the differentiation potential of such cells and the appropriateness of the protocol used to generate such cells. Other approaches may include the differentiation of iPSCs on a lung matrix to determine if the extracellular environment can facilitate the differentiation of the iPSCs into definitive endoderm and subsequently into lung endoderm (Gilpin et al., 2014). Eventually, a protocol will be needed that is capable of effectively differentiating a myriad of iPS cell lines, even if it may not be applicable to every single cell line. This would then create the possibility of applying the research to a number of lung diseases in addition to the bioengineering of lungs for transplantation in patients whose lungs are damaged beyond repair.

Figures

Figure 1: In vitro differentiation protocol for the differentiation of human induced pluripotent stem cells (iPSCs) into definitive endoderm, and subsequently, into lung endoderm.

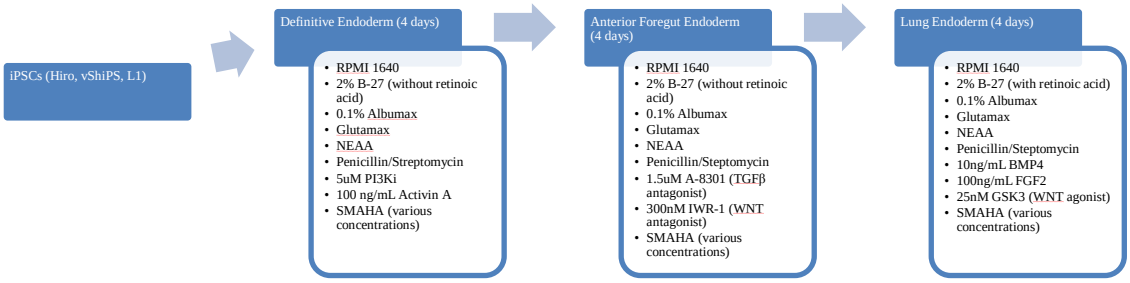

Figure 2: An increase in genes associated with the mesodermal and ectodermal lineage was observed in cells treated with SMAHA, with a decrease in endodermal gene expression. Quantitative polymerase chain reaction (qPCR) analysis on day 4 (differentiation to definitive endoderm) of differentiation relative to L1 undifferentiated day 0 cells (referred to as NC or negative control). qPCR data is expressed as a fold change (n = 6 separate experiments). The genes analyzed are as follows: A) FOXA2, B) SOX17, C) OCT-4, D) NANOG, E) CD34, F) CDH5, G) NCAM1, H) C-KIT, I) CXCR4, J) EPCAM, K) FOXA1, L) GATA4, and M) GATA6. The gene expression was normalized to GAPDH. Error bars represent the standard error of the mean (SEM). P-values < 0.05 were considered significant. P-values: * = <0.05, ** = <0.01, *** = <0.001, **** = <0.0001. NC = negative control (undifferentiated iPSCs), drug = SMAHA, Act = Activin.

A

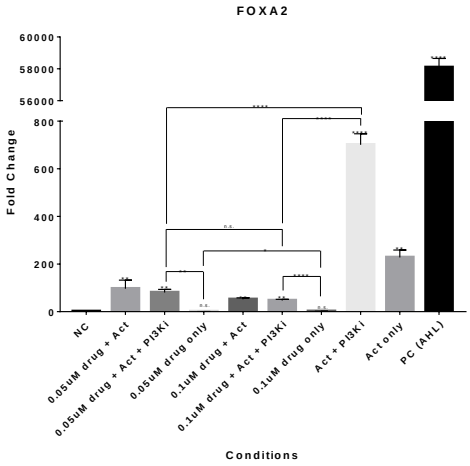

B

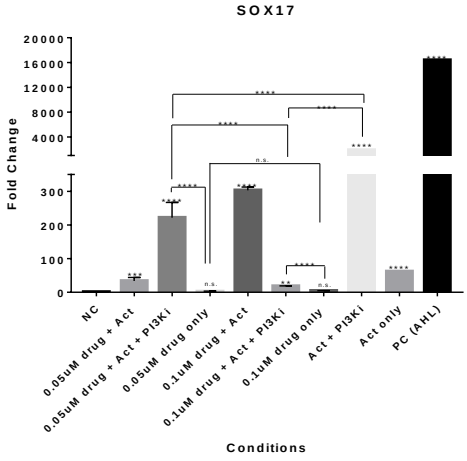

C

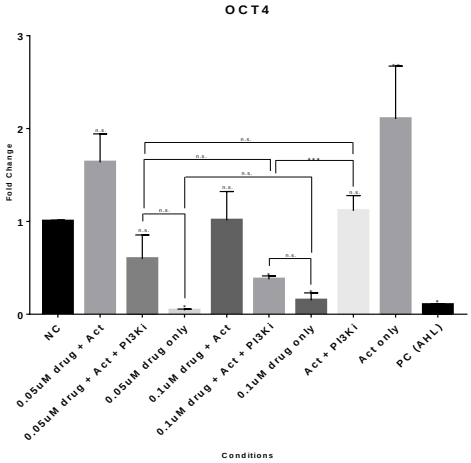

D

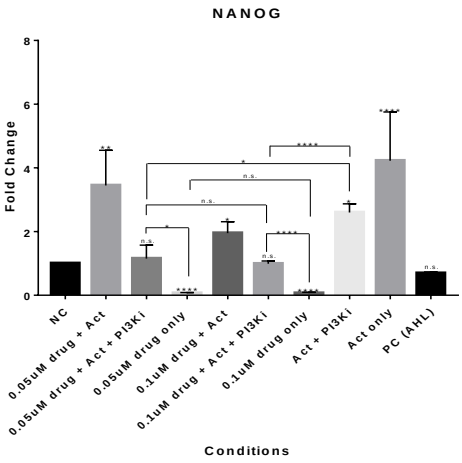

E

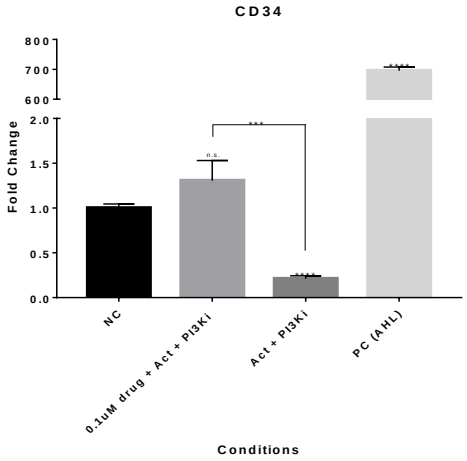
CD34
Fold Change
Conditions
NC
0.1uM drug + Act + PI3Ki
Act + PI3Ki
PC (AHL)

F

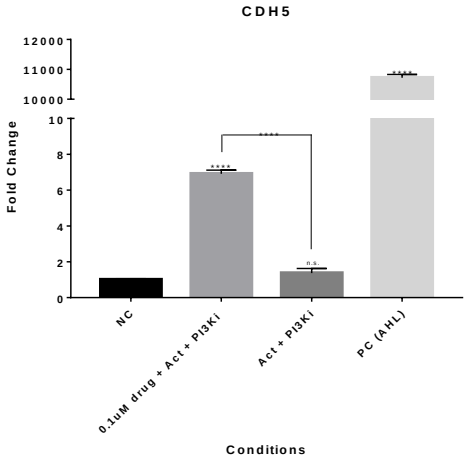
CDH5
Fold Change
Conditions
NC
0.1uM drug + Act + PI3Ki
Act + PI3Ki
PC (AHL)

G

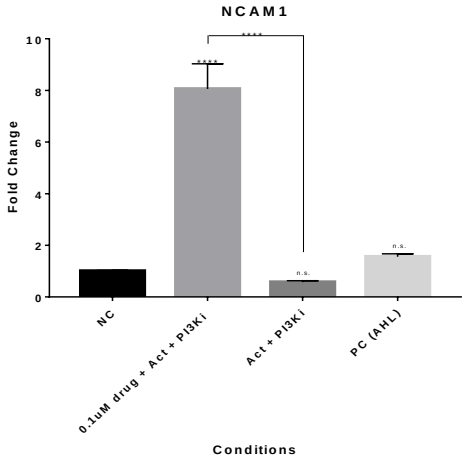
NCAM1
Fold Change
Conditions
NC
0.1uM drug + Act + PI3Ki
Act + PI3Ki
PC (AHL)

H

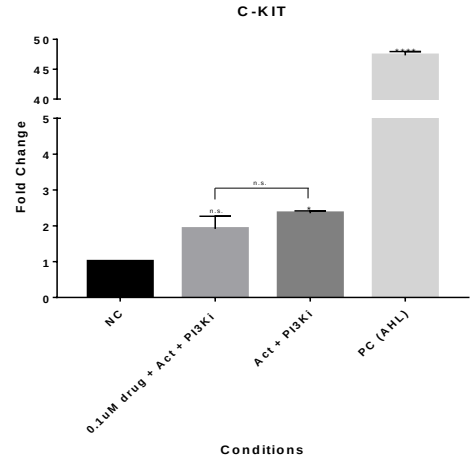
C-KIT
Fold Change
Conditions
NC
0.1uM drug + Act + PI3Ki
Act + PI3Ki
PC (AHL)

I

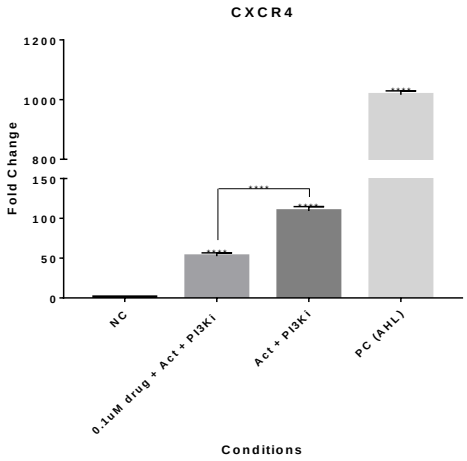
CXCR4
Fold Change
Conditions
NC
0.1uM drug + Act + PI3Ki
Act + PI3Ki
PC (AHL)

J

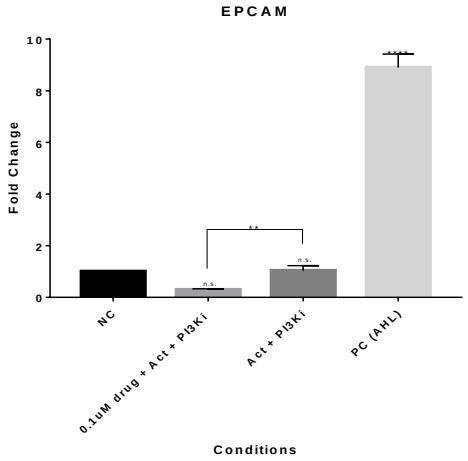
EPCAM
Fold Change
Conditions
NC
0.1uM drug + Act + PI3Ki
Act + PI3Ki
PC (AHL)

K

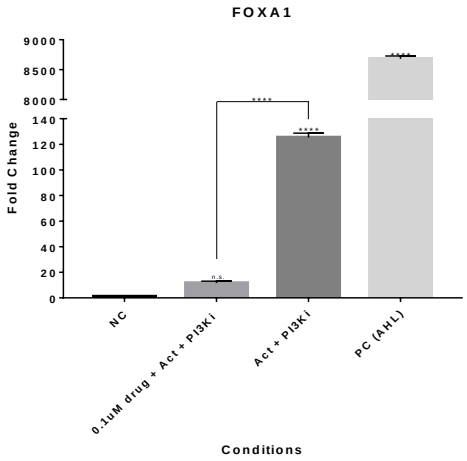
FOXA1
Fold Change
9000
8500
8000
140
120
100
80
60
40
20
0
****
****
n.s.
NC
0.1uM drug + Act + PI3Ki
Act + PI3Ki
PC (AHL)
Conditions

L

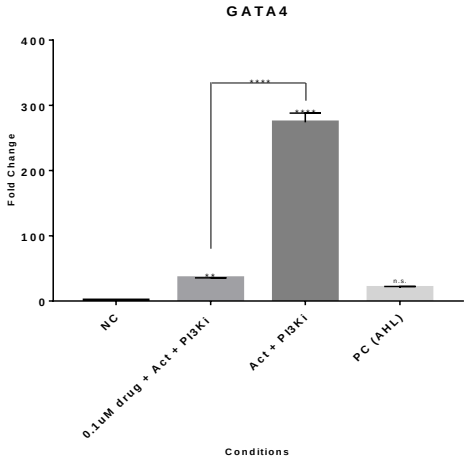
GATA4
Fold Change
400
300
200
100
0
****
****
**
n.s.
NC
0.1uM drug + Act + PI3Ki
Act + PI3Ki
PC (AHL)
Conditions

M

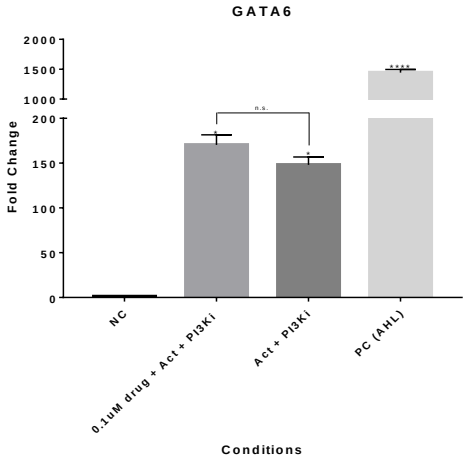
GATA6
Fold Change
2000
1500
1000
200
150
100
50
0
****
n.s.
*
NC
0.1uM drug + Act + PI3Ki
Act + PI3Ki
PC (AHL)
Conditions

Figure 3: L1 cells treated with SMAHA had fewer cells coexpressing the endodermal genes FOXA2 and SOX17 than those that were not treated with SMAHA. Flow cytometry and fluorescent images showing expression of pluripotent and definitive endoderm genes, in cells cultured according to protocol.
A) Expression of NANOG and OCT-4 in undifferentiated L1 cells,
B) Expression of FOXA2 in undifferentiated L1 cells,
C) Expression of SOX17 in undifferentiated L1 cells,
D) Flow cytometry data examining coexpression of FOXA2 and SOX17 in undifferentiated L1 cells,
E) Expression of FOXA2 in L1 cells cultured with SMAHA to induce definitive endoderm,
F) Expression of FOXA2 in L1 cells cultured without SMAHA to induce definitive endoderm,
G) Expression of SOX17 in L1 cells cultured with SMAHA to induce definitive endoderm,
H) Expression of SOX17 in L1 cells cultured without SMAHA to induce definitive endoderm,
I) Expression of NANOG in L1 cells cultured with SMAHA to induce definitive endoderm,
J) Expression of NANOG in L1 cells cultured without SMAHA to induce definitive endoderm,
K) Expression of OCT-4 in L1 cells cultured with SMAHA to induce definitive endoderm,
L) Expression of OCT-4 in L1 cells cultured without SMAHA to induce definitive endoderm
M) Flow cytometry data examining coexpression of FOXA2 and SOX17 in L1 cells cultured with SMAHA to induce definitive endoderm,
N) Flow cytometry data examining coexpression of FOXA2 and SOX17 in L1 cells cultured without SMAHA to induce definitive endoderm,
Scale bars = 100 um

A. Expression of NANOG and OCT-4 in undifferentiated L1 cells

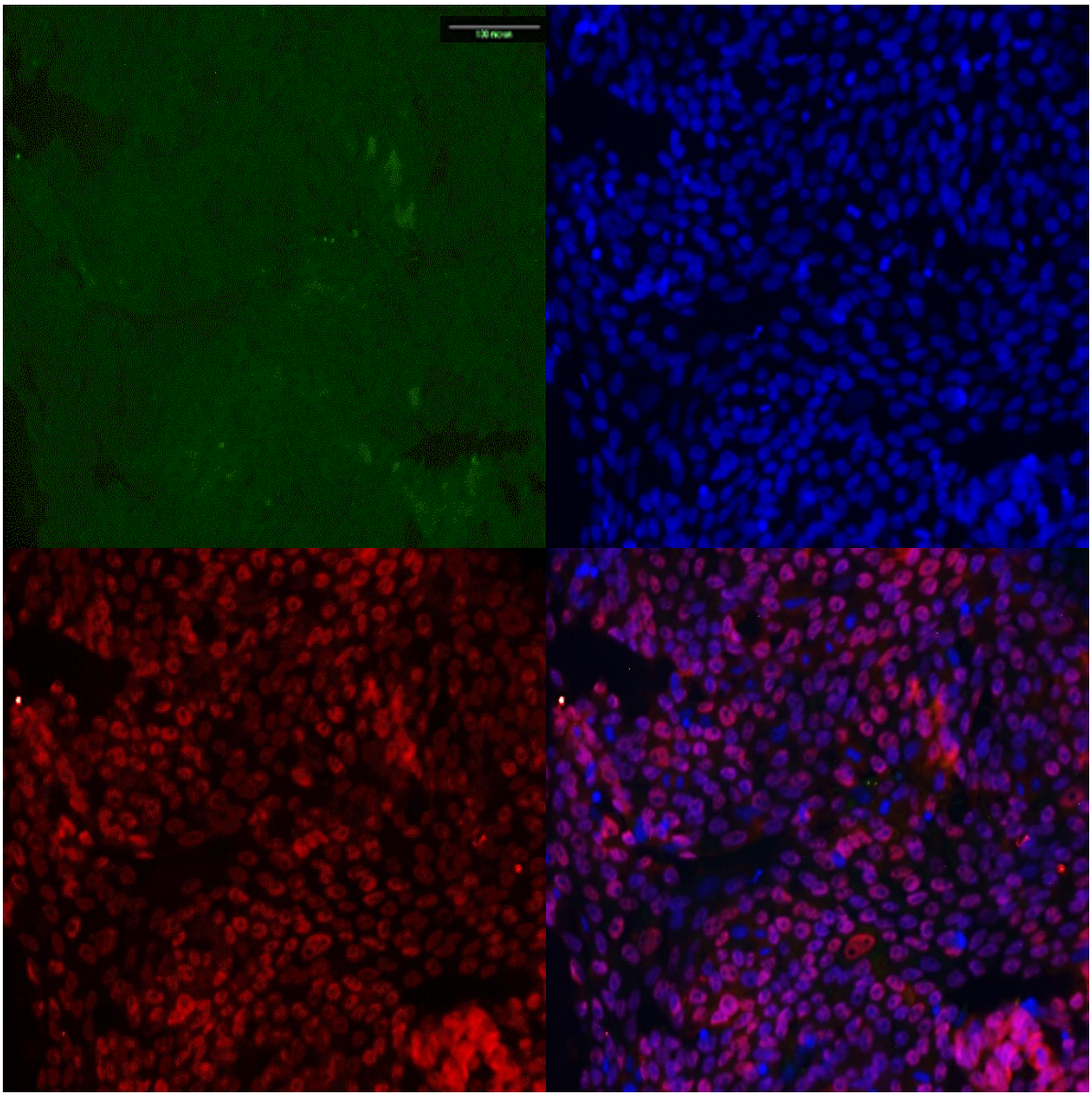

NANOG	DAPI
OCT4	MERGED

B. Expression of FOXA2 in undifferentiated L1 cells

FOXA2 DAPI MERGED

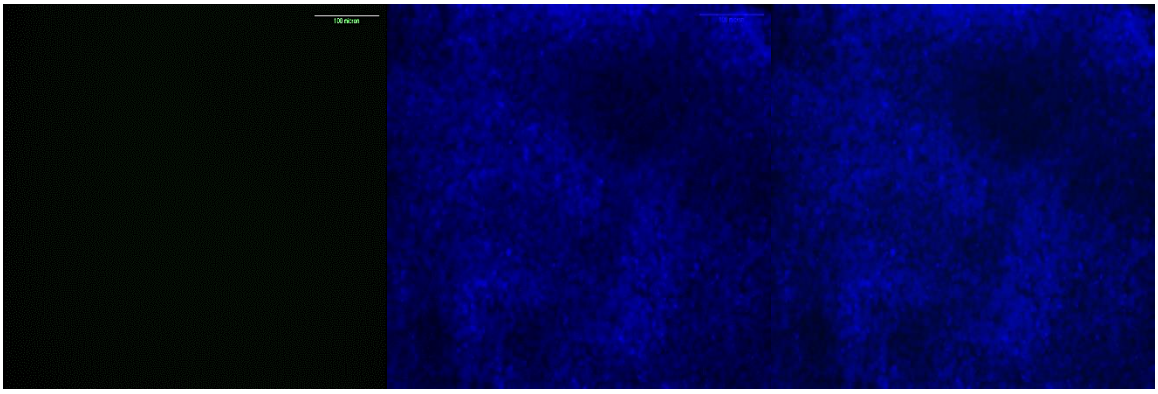

C. Expression of SOX17 in undifferentiated L1 cells

SOX17 DAPI MERGED

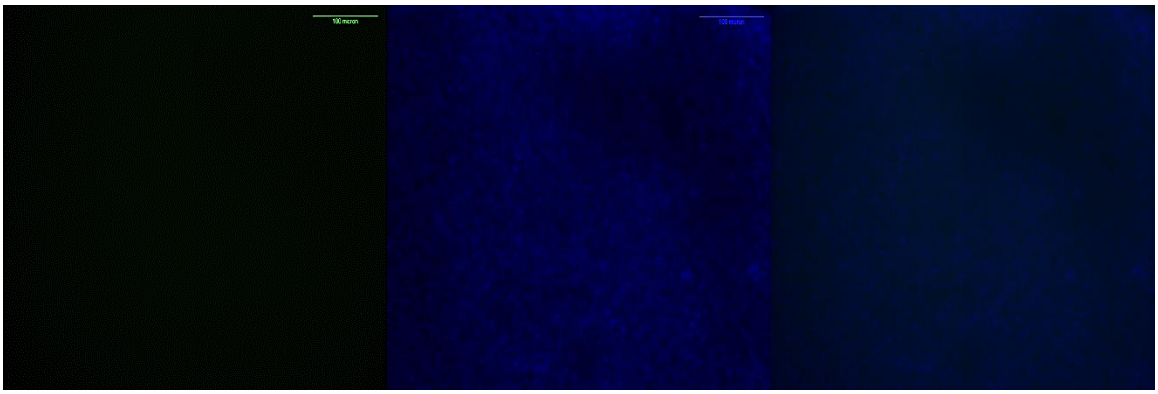

D. Flow cytometry data examining coexpression of FOXA2 and SOX17 in undifferentiated L1 cells

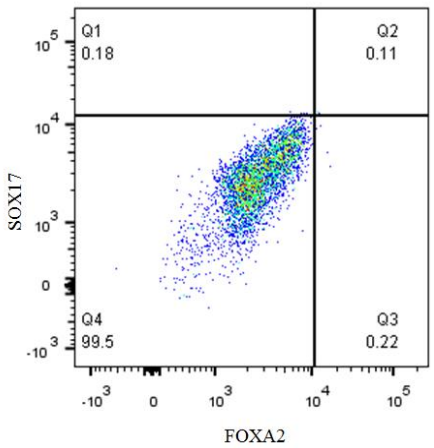

E. Expression of FOXA2 in L1 cells cultured with SMAHA to induce definitive endoderm

FOXA2 DAPI MERGED

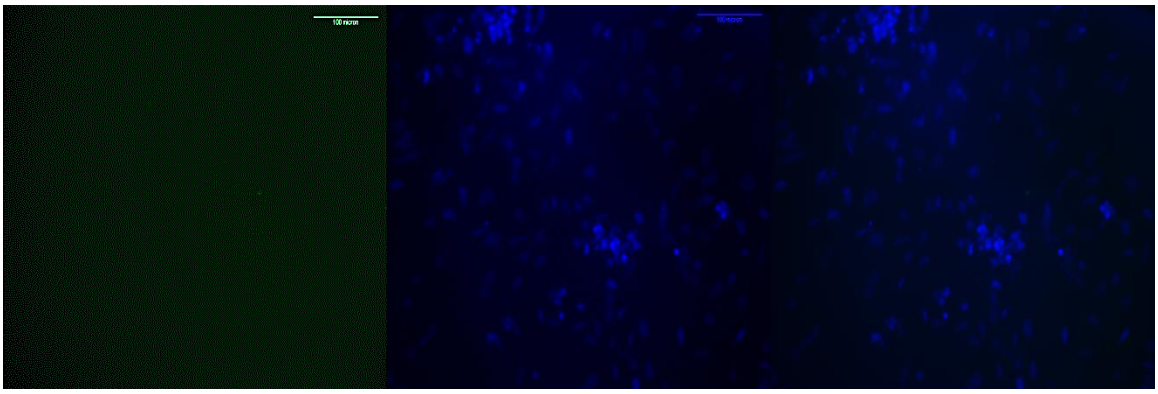

F. Expression of FOXA2 in L1 cells cultured without SMAHA to induce definitive endoderm

FOXA2 DAPI MERGED

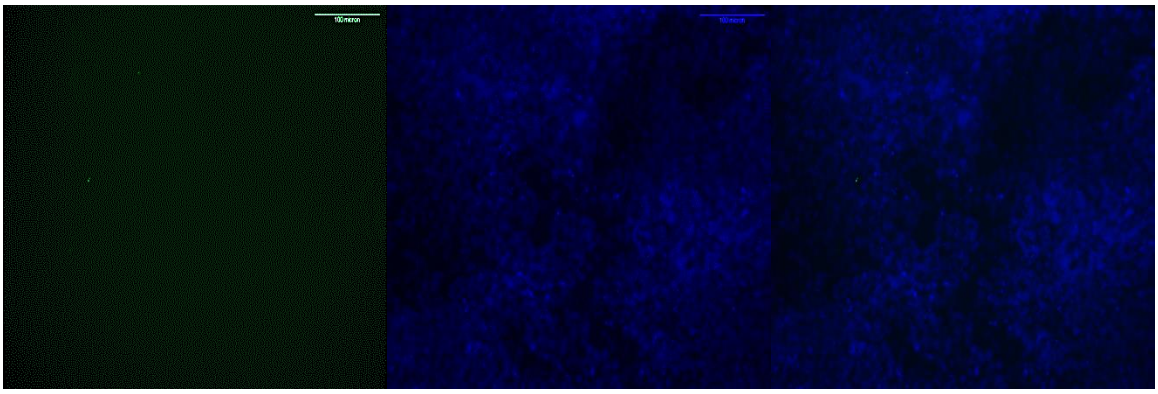

G. Expression of SOX17 in L1 cells cultured with SMAHA to induce definitive endoderm

SOX17 DAPI MERGED

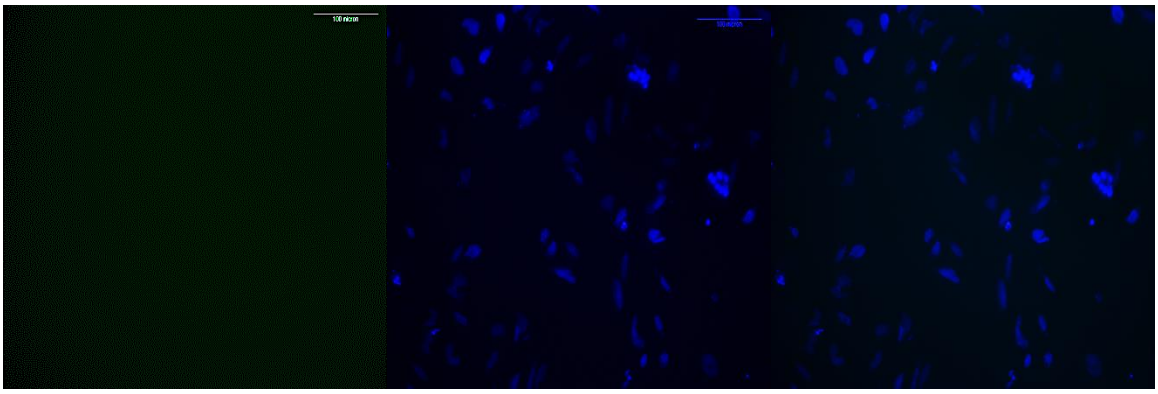

H. Expression of SOX17 in L1 cells cultured without SMAHA to induce definitive endoderm

SOX17 DAPI MERGED

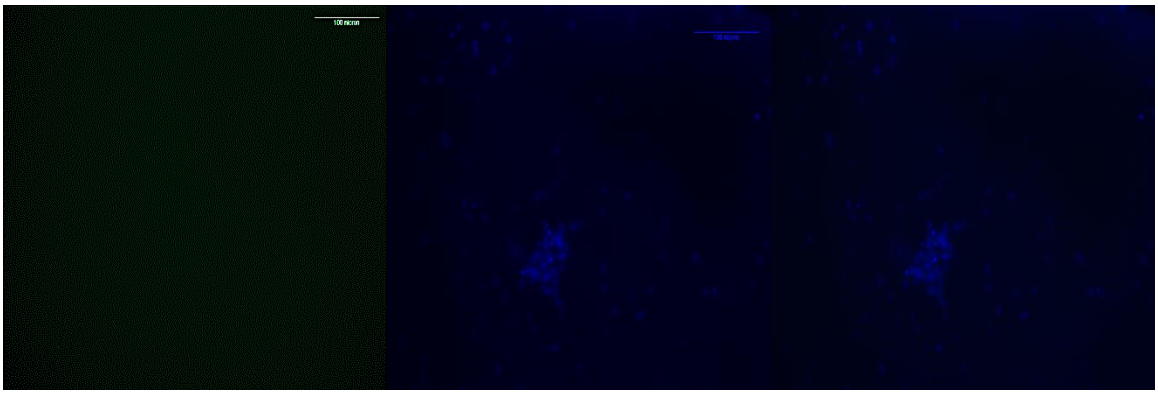

I. Expression of NANOG in L1 cells cultured with SMAHA to induce definitive endoderm

NANOG DAPI MERGED

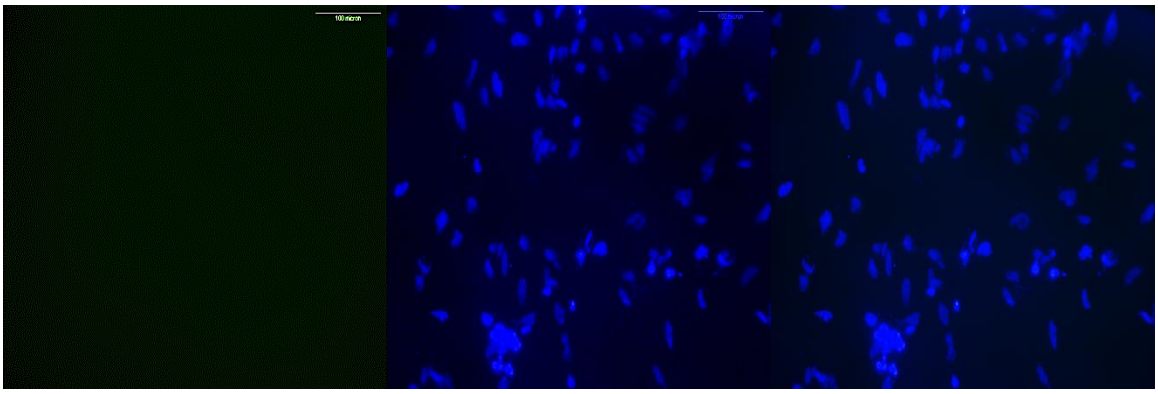

J. Expression of NANOG in L1 cells cultured without SMAHA to induce definitive endoderm

NANOG DAPI MERGED

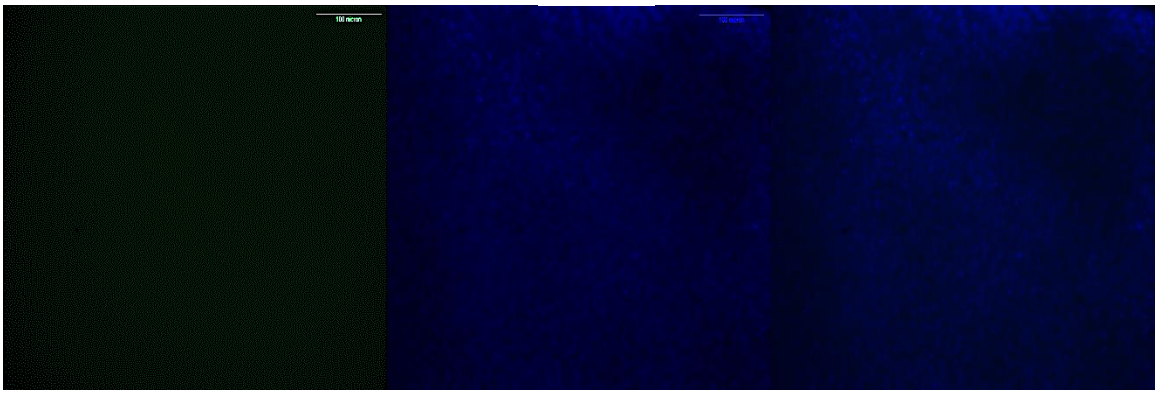

K. Expression of OCT-4 in L1 cells cultured with SMAHA to induce definitive endoderm

OCT-4 DAPI MERGED

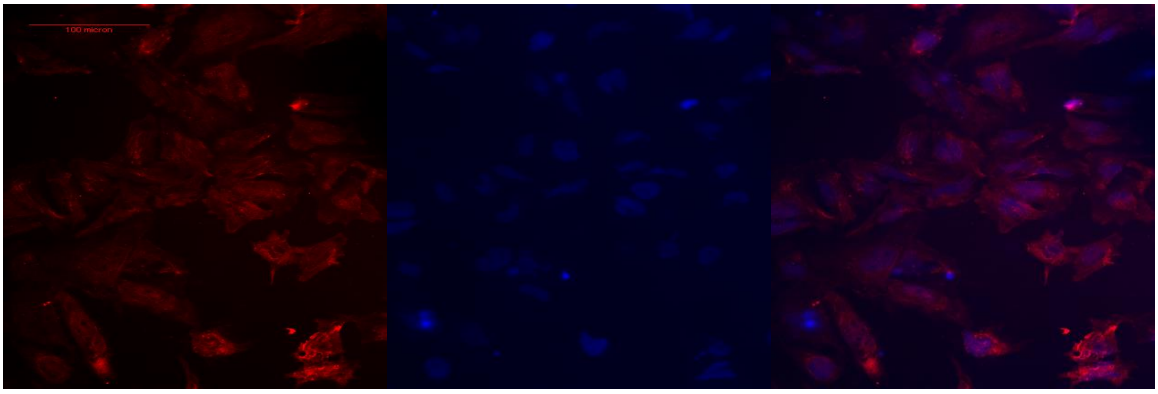

L. Expression of OCT-4 in L1 cells cultured without SMAHA to induce definitive endoderm

OCT-4 DAPI MERGED

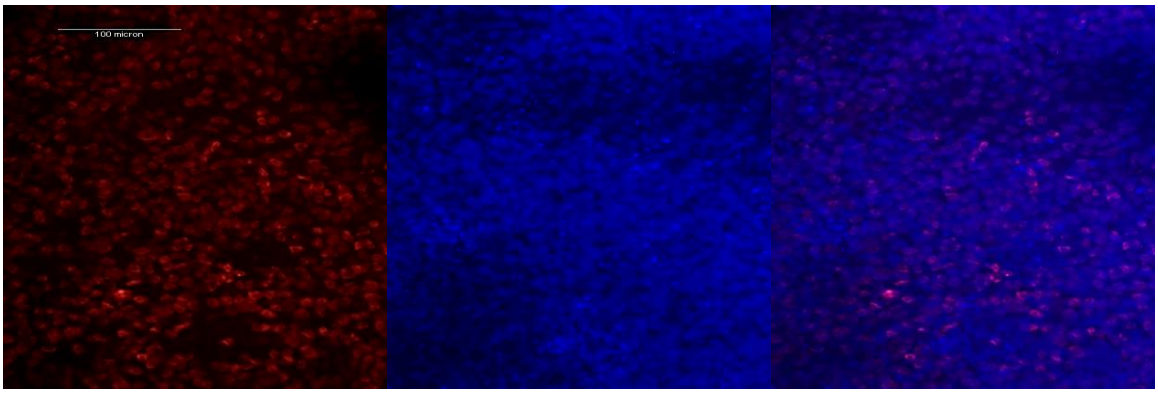

Flow cytometry data examining coexpression of FOXA2 and SOX17 in L1 cells cultured with SMAHA (Figure M) or without SMAHA (Figure N) to induce definitive endoderm

M

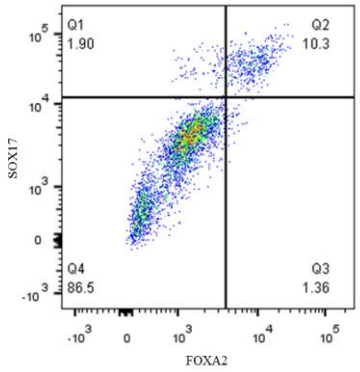

N

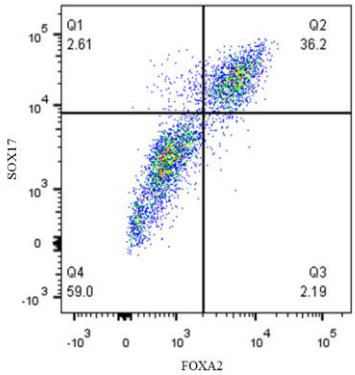

Figure 4: A decrease in cell quantity was observed when cells were cultured in the presence of SMAHA. Morphology of L1 cells that were induced into definitive endoderm when exposed to the given culture conditions for 4 days. All images are at 20x magnification. Scale bar = 200um

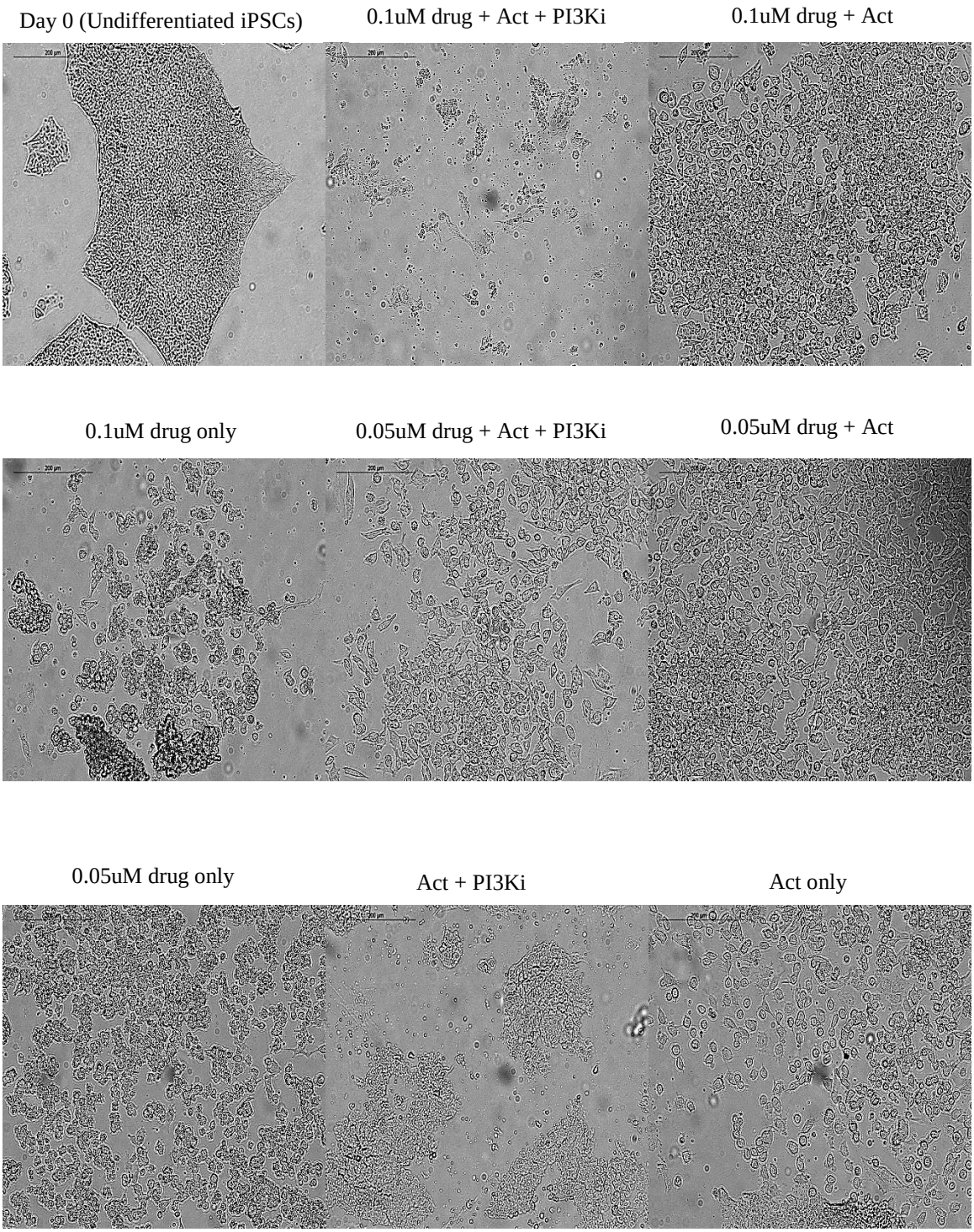

Figure 5: An increase in genes associated with the endodermal lineage, specifically FOXA2 and SOX17 was observed in cells treated with SMAHA, and DMSO also seemed to have an effect on the expression of various genes. Quantitative polymerase chain reaction (qPCR) analysis on day 4 (differentiation to definitive endoderm) of differentiation relative to Hiro undifferentiated day 0 cells (referred to as NC or negative control). qPCR data is expressed as a fold change (n = 5 separate experiments). The genes analyzed are as follows: A) FOXA2, B) SOX17, C) OCT-4, D) NANOG, E) CD34, F) CDH5, G) NCAM1, H) CXCR4, I) C-KIT, J) EPCAM, K) FOXA1, L) GATA4, M) GATA6, and N) NKX2.1. The gene expression was normalized to GAPDH. Error bars represent the standard error of the mean (SEM). P-values < 0.05 were considered significant. P-values: * = <0.05, ** = <0.01, *** = <0.001, **** = <0.0001. NC = negative control (undifferentiated iPSCs), drug = SMAHA, Act = Activin.

A

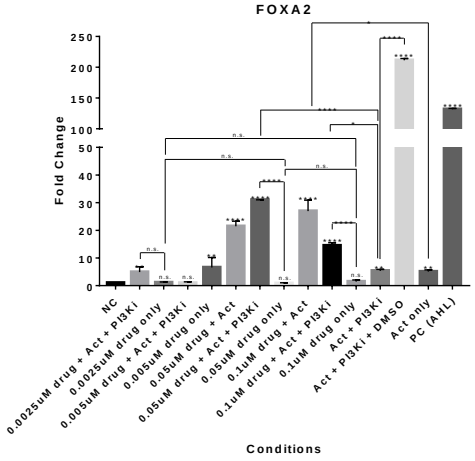

B

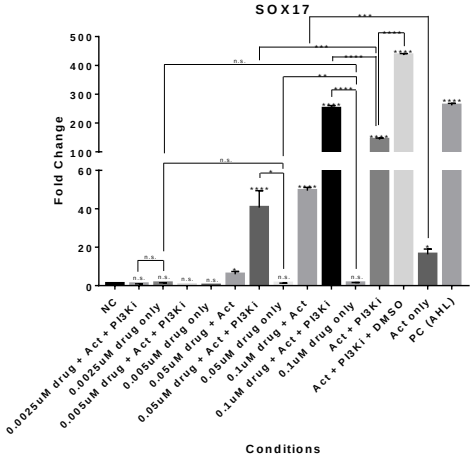

C

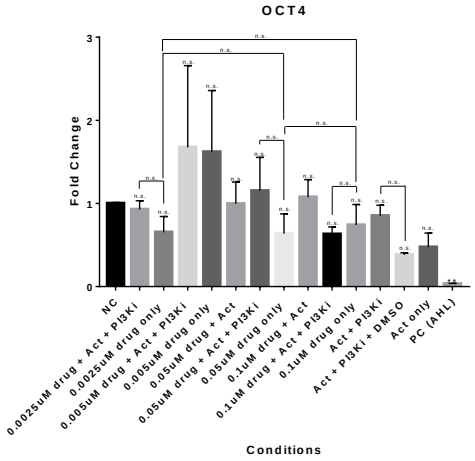

D

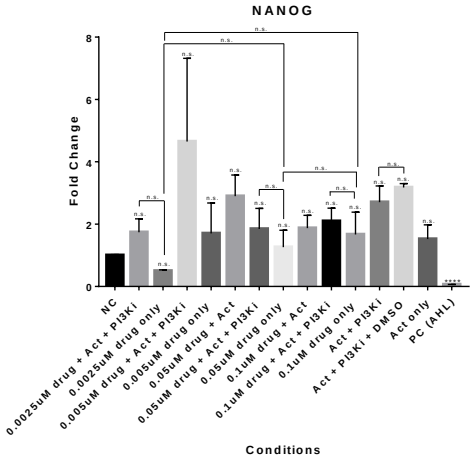

E

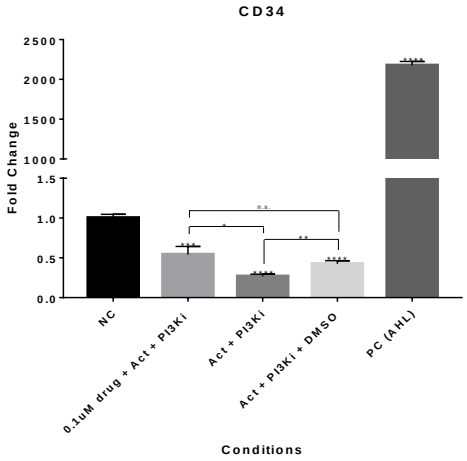
CD34
Fold Change
2500
2000
1500
1000
1.5
1.0
0.5
0.0
n.s.
*
**
****
NC
0.1uM drug + Act + PI3Ki
Act + PI3Ki
Act + PI3Ki + DMSO
PC (AHL)
Conditions

F

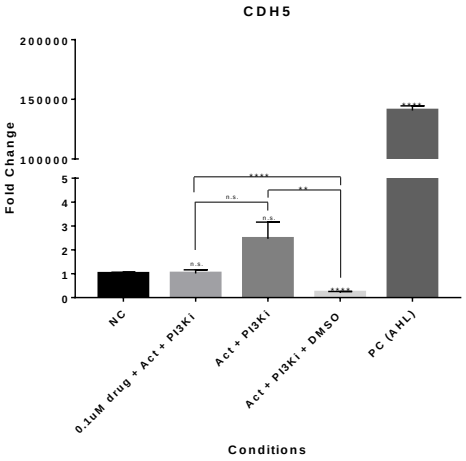
CDH5
Fold Change
200000
150000
100000
5
4
3
2
1
0
****
n.s.
**
NC
0.1uM drug + Act + PI3Ki
Act + PI3Ki
Act + PI3Ki + DMSO
PC (AHL)
Conditions

G

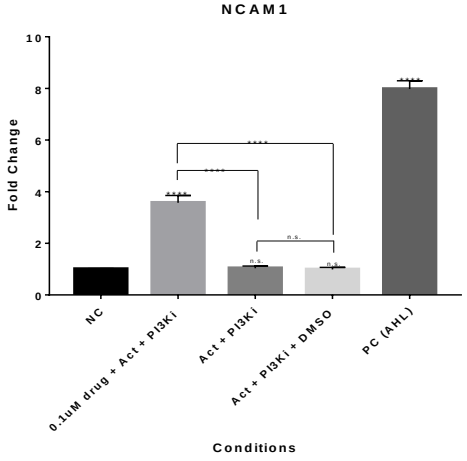
NCAM1
Fold Change
10
8
6
4
2
0
****
****
n.s.
n.s.
NC
0.1uM drug + Act + PI3Ki
Act + PI3Ki
Act + PI3Ki + DMSO
PC (AHL)
Conditions

H

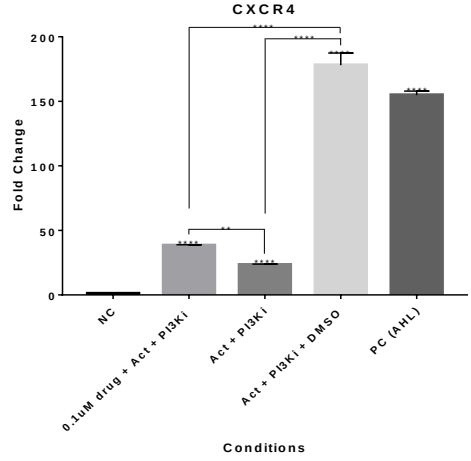
CXCR4
Fold Change
200
150
100
50
0
****
****
**
NC
0.1uM drug + Act + PI3Ki
Act + PI3Ki
Act + PI3Ki + DMSO
PC (AHL)
Conditions

I

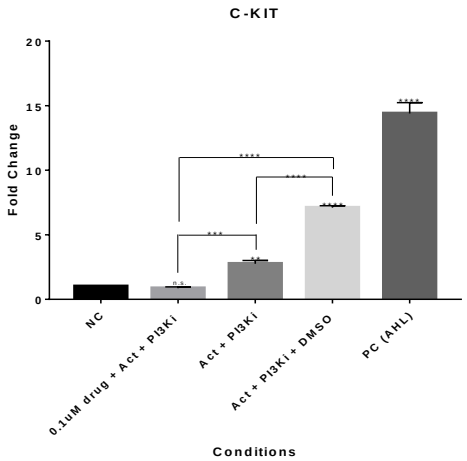
C-KIT
Fold Change
20
15
10
5
0
****
****
***
n.s.
NC
0.1uM drug + Act + PI3Ki
Act + PI3Ki
Act + PI3Ki + DMSO
PC (AHL)
Conditions

J

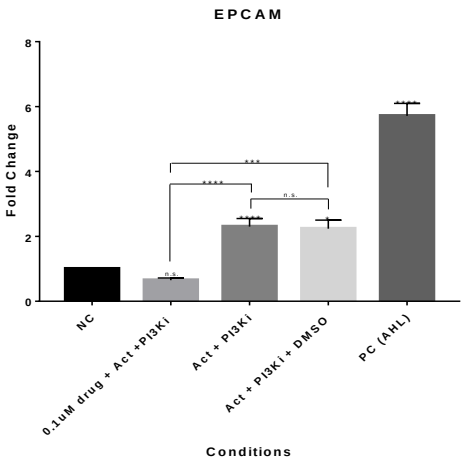
EPCAM
Fold Change
8
6
4
2
0
***
****
n.s.
NC
0.1uM drug + Act + PI3Ki
Act + PI3Ki
Act + PI3Ki + DMSO
PC (AHL)
Conditions

K

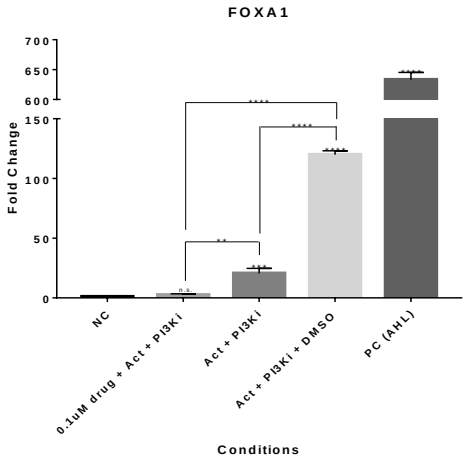
FOXA1
Fold Change
700
650
600
150
100
50
0
NC
0.1uM drug + Act + PI3Ki
Act + PI3Ki
Act + PI3Ki + DMSO
PC (AHL)
Conditions

L

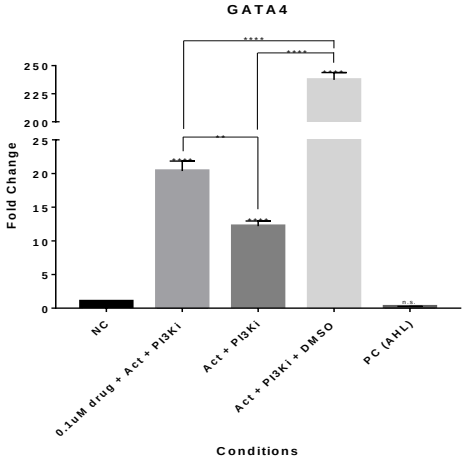
GATA4
Fold Change
250
225
200
25
20
15
10
5
0
NC
0.1uM drug + Act + PI3Ki
Act + PI3Ki
Act + PI3Ki + DMSO
PC (AHL)
Conditions

M

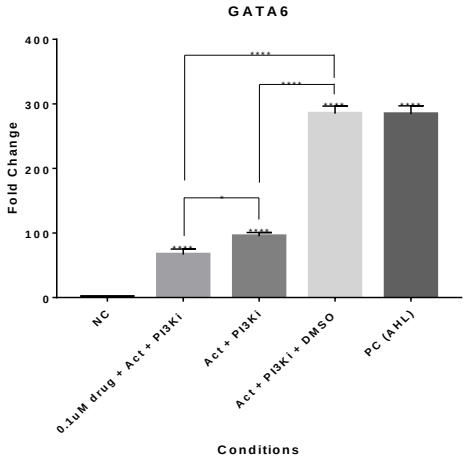
GATA6
Fold Change
400
300
200
100
0
NC
0.1uM drug + Act + PI3Ki
Act + PI3Ki
Act + PI3Ki + DMSO
PC (AHL)
Conditions

N

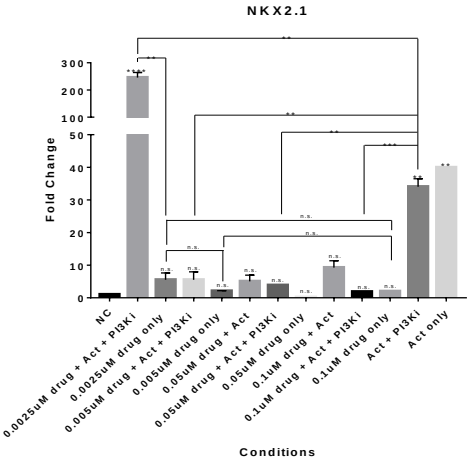
NKX2.1
Fold Change
300
200
100
50
40
30
20
10
0
NC
PI3Ki
0.0025uM drug + Act + PI3Ki
0.0025uM drug only
0.005uM drug + Act + PI3Ki
0.005uM drug only
0.05uM drug + Act
0.05uM drug + Act + PI3Ki
0.05uM drug only
0.1uM drug + Act
0.1uM drug + Act + PI3Ki
0.1uM drug only
Act + PI3Ki
Act only
Conditions

Figure 6: Hiro cells treated with SMAHA had a greater percentage of cells coexpressing the endodermal genes FOXA2 and SOX17 than those that were not treated with SMAHA. Flow cytometry and fluorescent images showing expression of pluripotent and definitive endoderm genes, in cells cultured according to protocol.
A) Expression of NANOG and OCT-4 in undifferentiated Hiro cells,
B) Expression of FOXA2 in undifferentiated Hiro cells,
C) Expression of SOX17 in undifferentiated Hiro cells,
D) Flow cytometry data examining coexpression of FOXA2 and SOX17 in undifferentiated Hiro cells,
E) Expression of FOXA2 in Hiro cells cultured with SMAHA to induce definitive endoderm,
F) Expression of FOXA2 in Hiro cells cultured without SMAHA to induce definitive endoderm,
G) Expression of SOX17 in Hiro cells cultured with SMAHA to induce definitive endoderm,
H) Expression of SOX17 in Hiro cells cultured without SMAHA to induce definitive endoderm,
I) Expression of NANOG in Hiro cells cultured with SMAHA to induce definitive endoderm,
J) Expression of NANOG in Hiro cells cultured without SMAHA to induce definitive endoderm,
K) Expression of OCT-4 in Hiro cells cultured with SMAHA to induce definitive endoderm,
L) Expression of OCT-4 in Hiro cells cultured without SMAHA to induce definitive endoderm,
M) Flow cytometry data examining coexpression of FOXA2 and SOX17 in Hiro cells cultured with SMAHA to induce definitive endoderm,
N) Flow cytometry data examining coexpression of FOXA2 and SOX17 in Hiro cells cultured without SMAHA to induce definitive endoderm
Scale bars = 100 um

A. Expression of NANOG and OCT-4 in undifferentiated Hiro cells

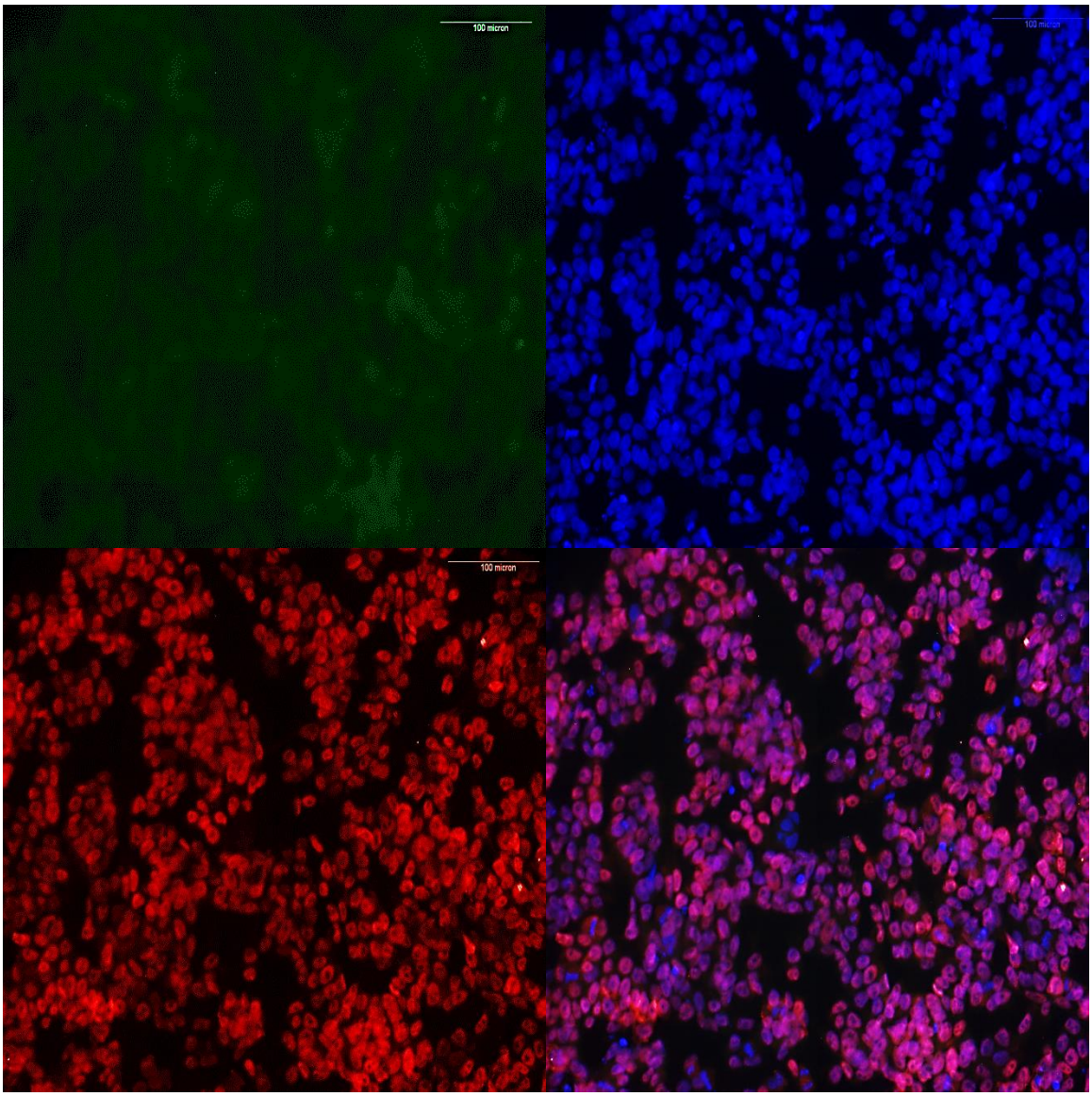

NANOG	DAPI
OCT4	MERGED

B. Expression of FOXA2 in undifferentiated Hiro cells

FOXA2 DAPI MERGED

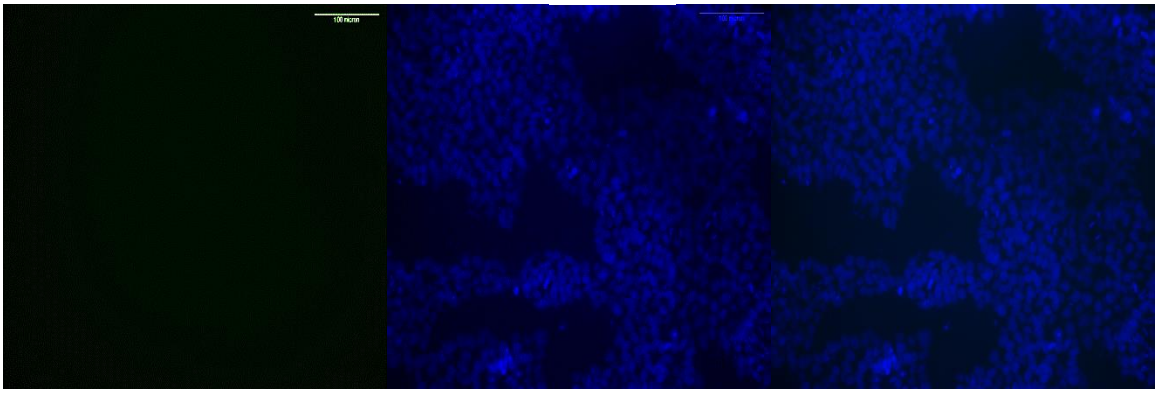

C. Expression of SOX17 in undifferentiated Hiro cells

SOX17 DAPI MERGED

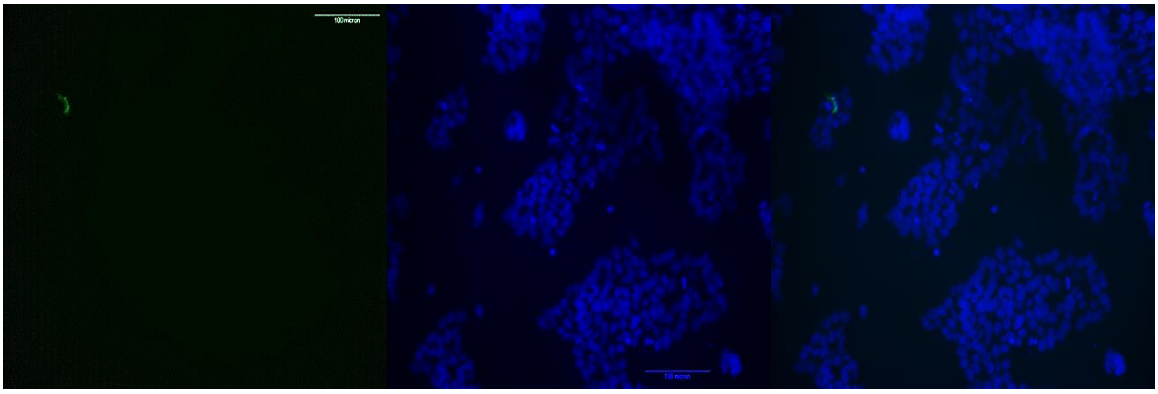

D. Flow cytometry data examining coexpression of FOXA2 and SOX17 in undifferentiated Hiro cells

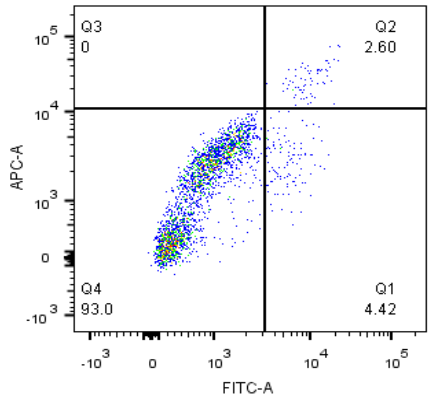

E. Expression of FOXA2 in Hiro cells cultured with SMAHA to induce definitive endoderm

FOXA2 DAPI MERGED

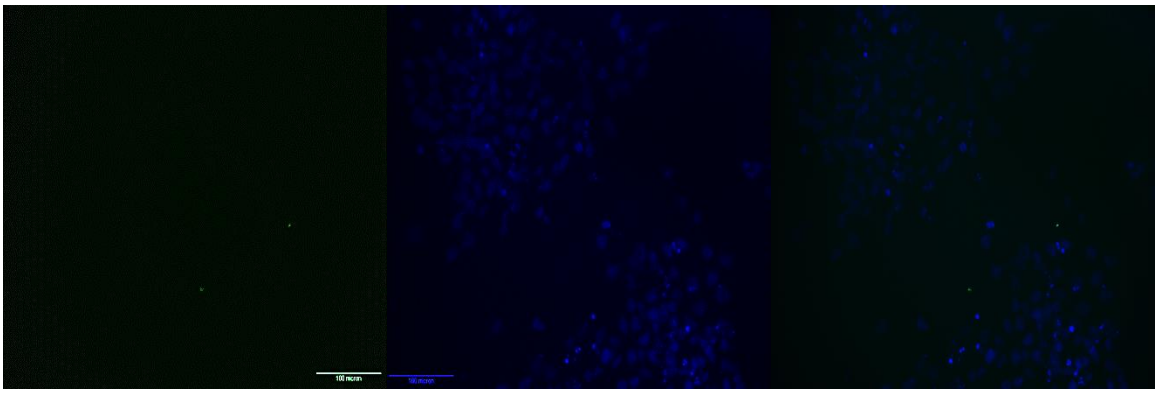

F. Expression of FOXA2 in Hiro cells cultured without SMAHA to induce definitive endoderm

FOXA2 DAPI MERGED

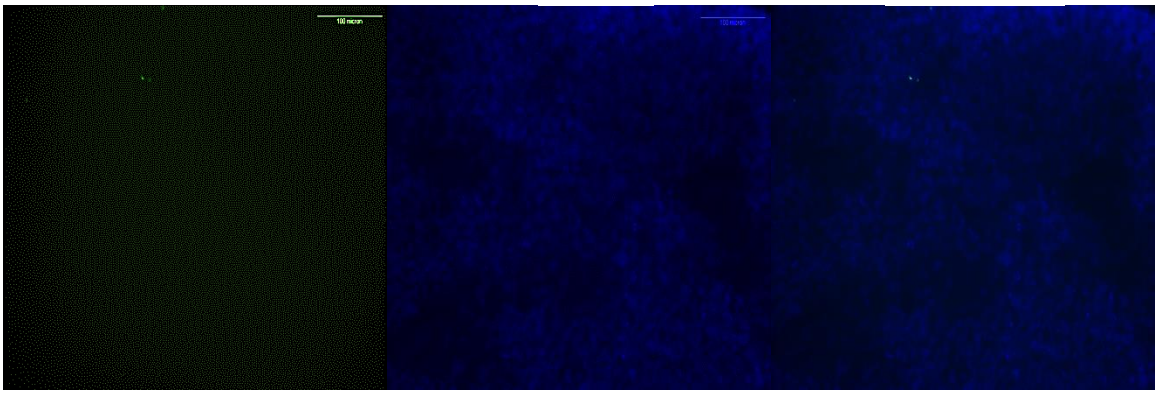

G. Expression of SOX17 in Hiro cells cultured with SMAHA to induce definitive endoderm

SOX17 DAPI MERGED

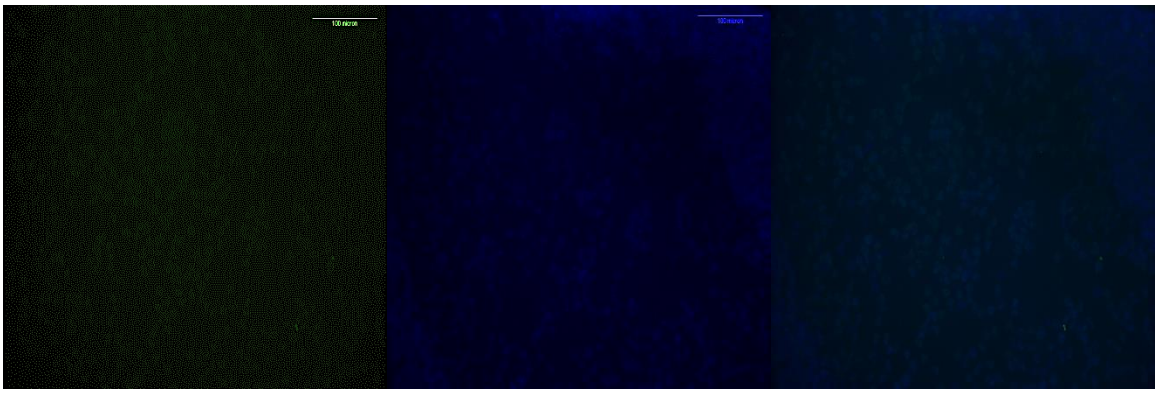

H. Expression of SOX17 in Hiro cells cultured without SMAHA to induce definitive endoderm

SOX17 DAPI MERGED

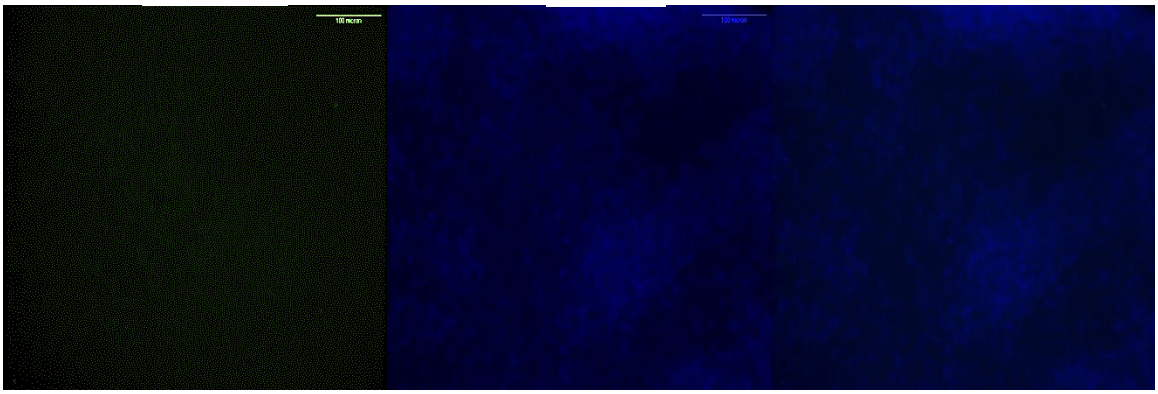

I. Expression of NANOG in Hiro cells cultured with SMAHA to induce definitive endoderm

NANOG DAPI MERGED

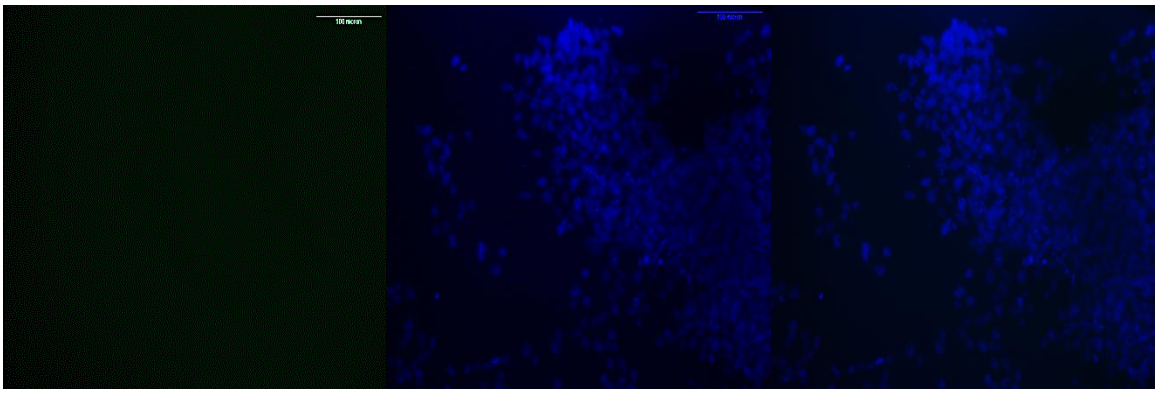

J. Expression of NANOG in Hiro cells cultured without SMAHA to induce definitive endoderm

NANOG DAPI MERGED

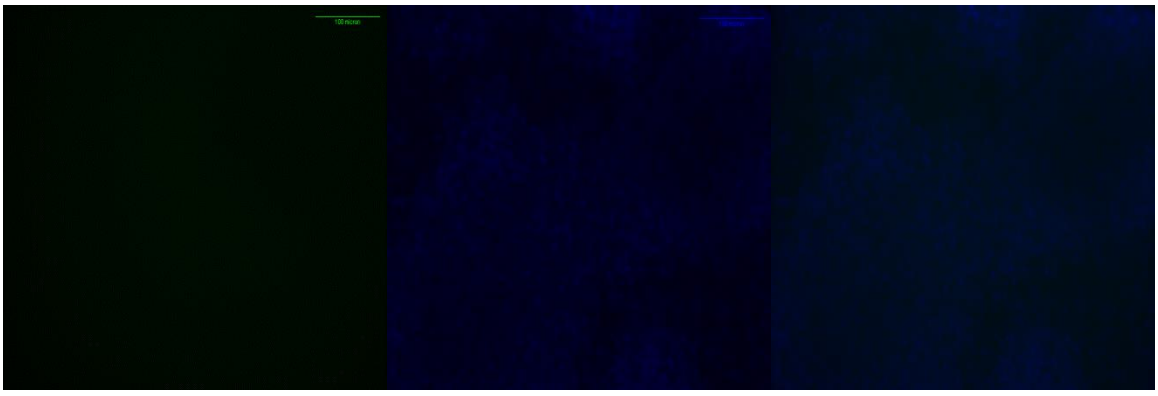

K. Expression of OCT-4 in Hiro cells cultured with SMAHA to induce definitive endoderm

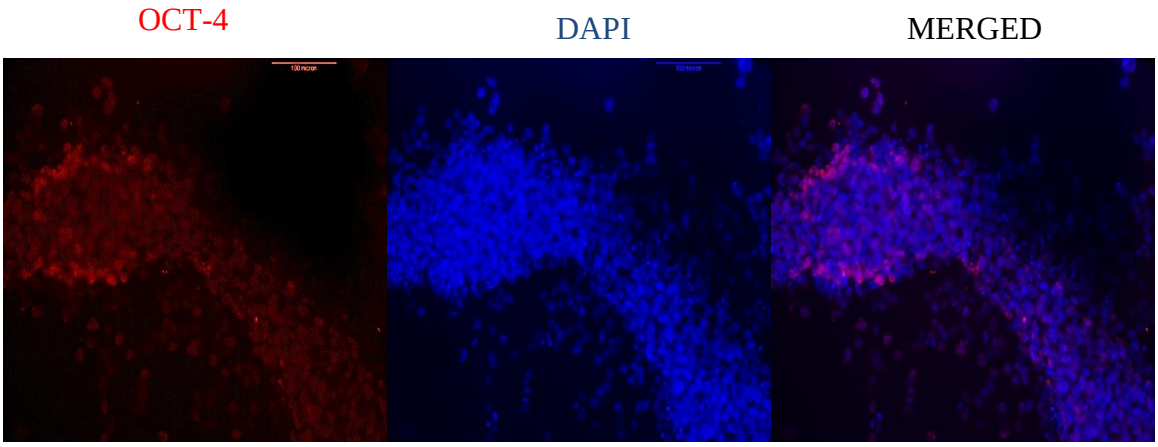

L. Expression of OCT-4 in Hiro cells cultured without SMAHA to induce definitive endoderm

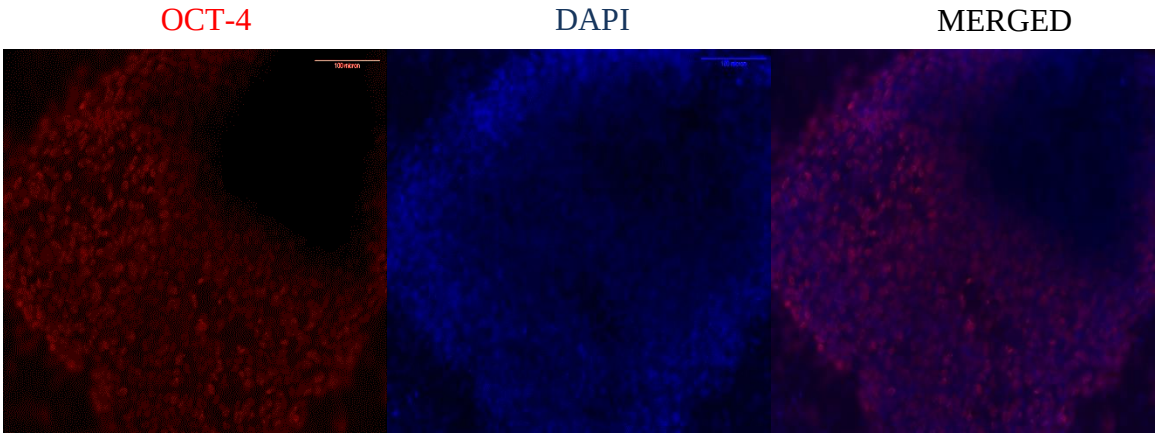

Flow cytometry data examining coexpression of FOXA2 and SOX17 in Hiro cells cultured with SMAHA (Figure M) or without SMAHA (Figure N) to induce definitive endoderm

M

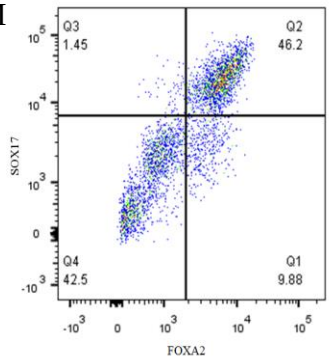

N

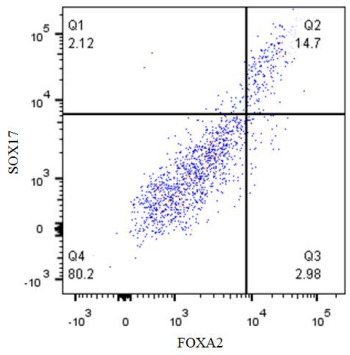

Figure 7: The morphology of Hiro cells did not seem to vary for the most part with the different culture conditions and the similar cell viabilities demonstrates that SMAHA was not toxic to the cells. Hiro cells were induced into definitive endoderm when exposed to the given culture conditions for 4 days. All images are at 20x magnification.
Scale bar = 200um

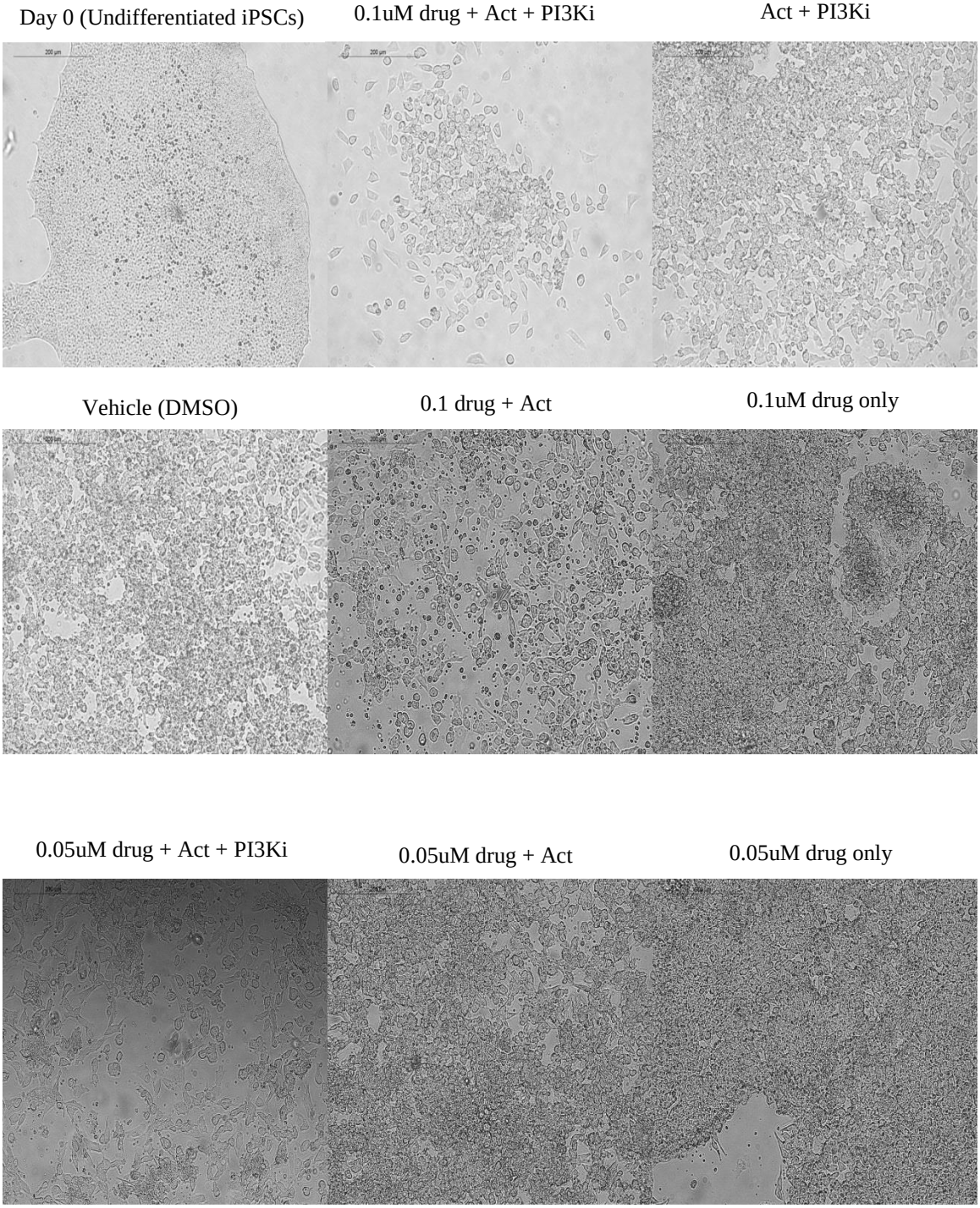

Act only

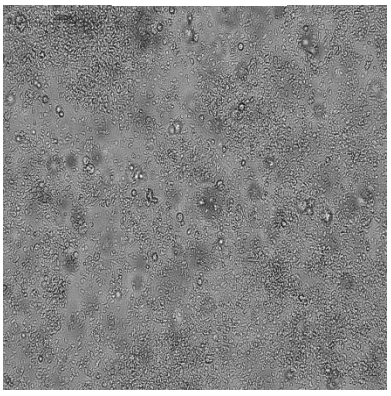

Figure 8: Flow cytometry showing expression of pluripotent and definitive endoderm genes, in cells cultured according to protocol.
A) Coexpression of CXCR4 and C-KIT in undifferentiated vShiPS cells,
B) vShiPS that were sorted for CXCR4+ expressing cells after four days of differentiation into definitive endoderm without SMAHA
C) Coexpression of FOXA2 and SOX17 in sorted definitive endoderm (CXCR4+) cells

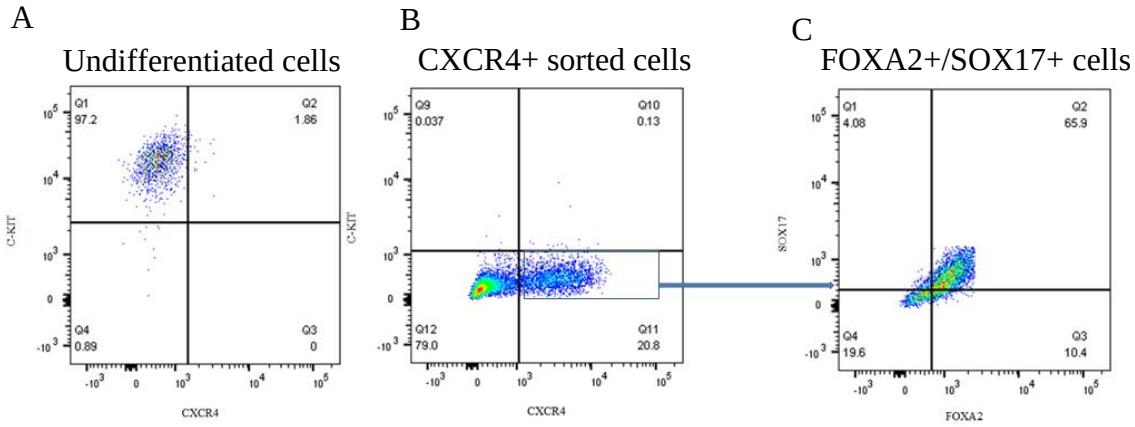

Figure 9: Overall, for each differentiation stage, cells treated with SMAHA led to a lower expression of the various genes examined. Quantitative polymerase chain reaction (qPCR) analysis of differentiations relative to vShiPS undifferentiated day 0 cells (referred to as NC or negative control). qPCR data is expressed as a fold change (n = 2 separate experiments). The genes analyzed are as follows: A) OCT-4, B) CDH5, C) C-KIT, D) CXCR4, E) EPCAM, F) FOXA1, G) FOXA2, H) GATA4, I) GATA6, J) NANOG, K) NCAM1, L) SOX17, M) CDX2, N) NKX2.1, and O) SOX2. The gene expression was normalized to GAPDH. Error bars represent the standard error of the mean (SEM). P-values < 0.05 were considered significant. P-values: * = <0.05, ** = <0.01, *** = <0.001, **** = <0.0001. NC = negative control (undifferentiated iPSCs), drug = SMAHA, Act = Activin.

A

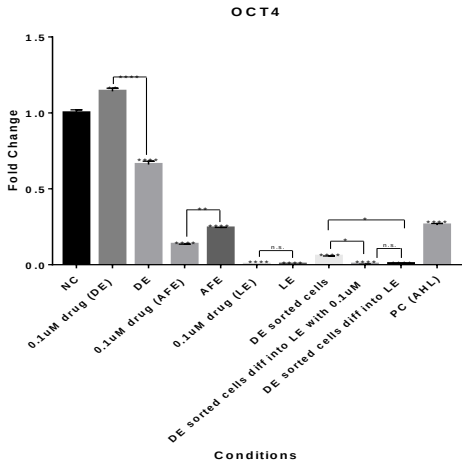

B

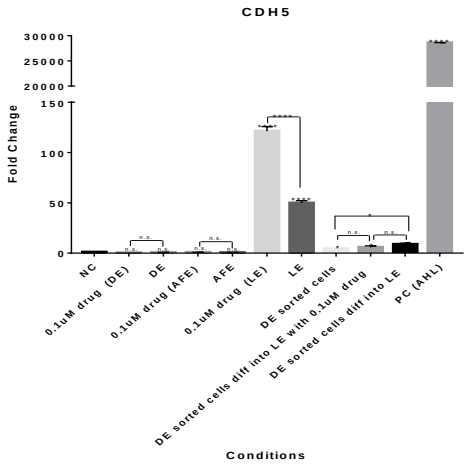

C

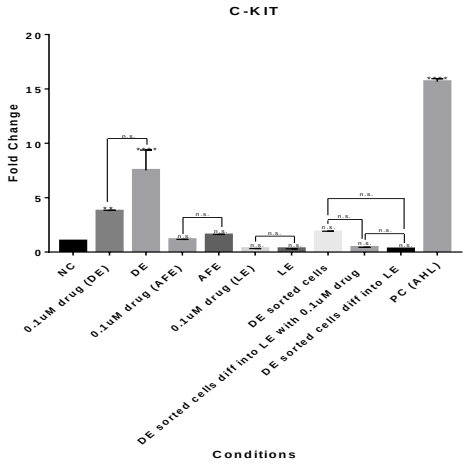

D

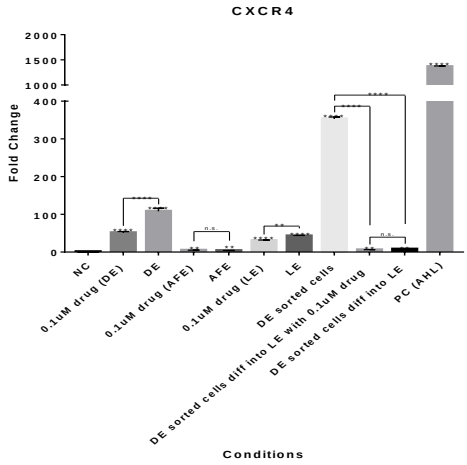

E

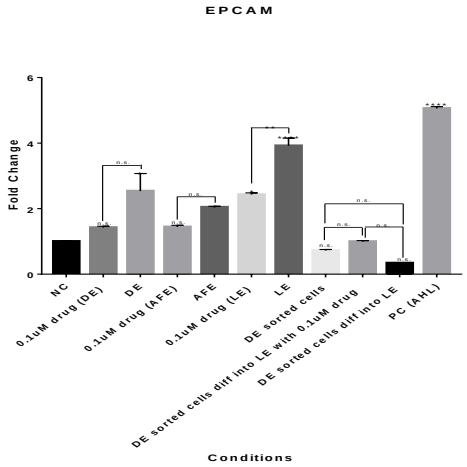
EPCAM
Fold Change
Conditions
NC
0.1uM drug (DE)
DE
0.1uM drug (AFE)
AFE
0.1uM drug (LE)
LE
DE sorted cells
DE sorted cells diff into LE with 0.1uM drug
DE sorted cells diff into LE
PC (AHL)

F

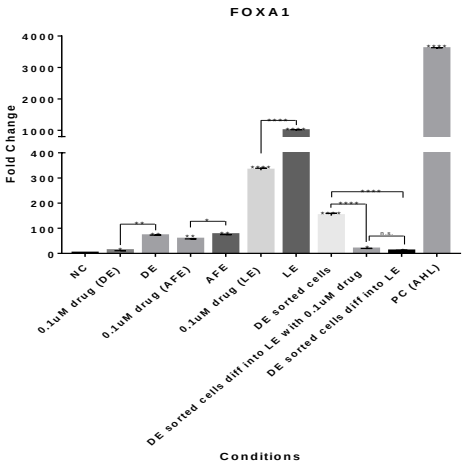
FOXA1
Fold Change
Conditions
NC
0.1uM drug (DE)
DE
0.1uM drug (AFE)
AFE
0.1uM drug (LE)
LE
DE sorted cells
DE sorted cells diff into LE with 0.1uM drug
DE sorted cells diff into LE
PC (AHL)

G

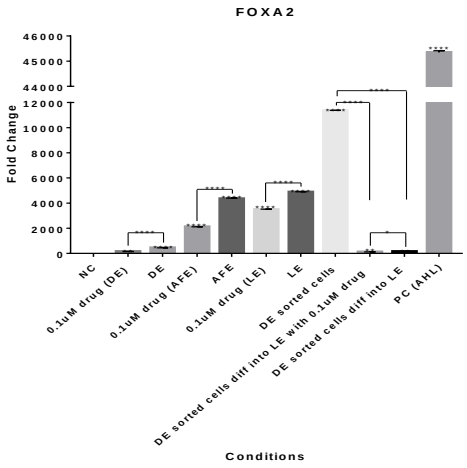
FOXA2
Fold Change
Conditions
NC
0.1uM drug (DE)
DE
0.1uM drug (AFE)
AFE
0.1uM drug (LE)
LE
DE sorted cells
DE sorted cells diff into LE with 0.1uM drug
DE sorted cells diff into LE
PC (AHL)

H

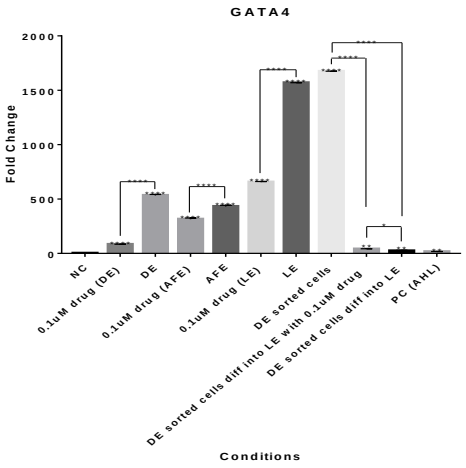
GATA4
Fold Change
Conditions
NC
0.1uM drug (DE)
DE
0.1uM drug (AFE)
AFE
0.1uM drug (LE)
LE
DE sorted cells
DE sorted cells diff into LE with 0.1uM drug
DE sorted cells diff into LE
PC (AHL)

I

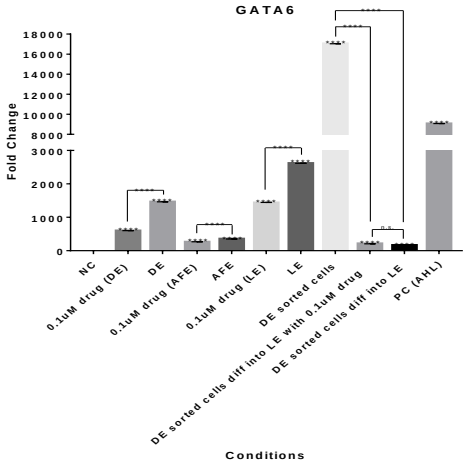
GATA6
Fold Change
Conditions
NC
0.1uM drug (DE)
DE
0.1uM drug (AFE)
AFE
0.1uM drug (LE)
LE
DE sorted cells
DE sorted cells diff into LE with 0.1uM drug
DE sorted cells diff into LE
PC (AHL)

J

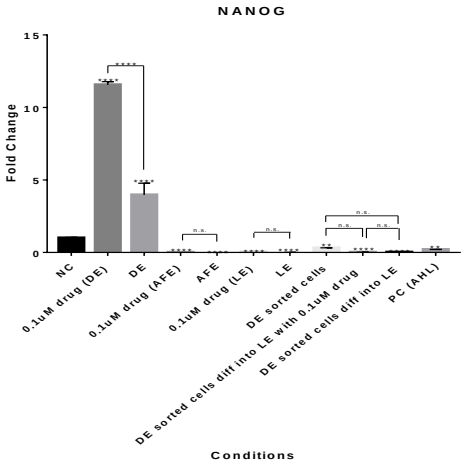
NANOG
Fold Change
Conditions
NC
0.1uM drug (DE)
DE
0.1uM drug (AFE)
AFE
0.1uM drug (LE)
LE
DE sorted cells
DE sorted cells diff into LE with 0.1uM drug
DE sorted cells diff into LE
PC (AHL)

K

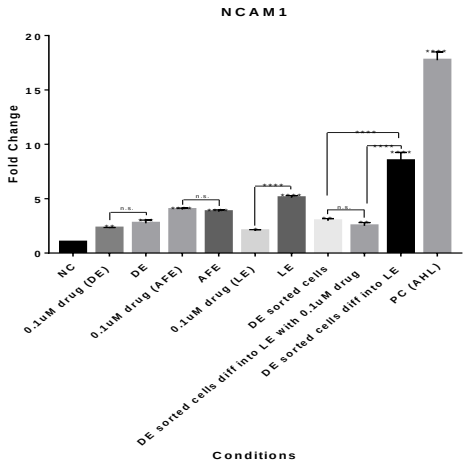
NCAM1
Fold Change
Conditions
NC
0.1uM drug (DE)
DE
0.1uM drug (AFE)
AFE
0.1uM drug (LE)
LE
DE sorted cells
DE sorted cells diff into LE with 0.1uM drug
DE sorted cells diff into LE
PC (AHL)

L

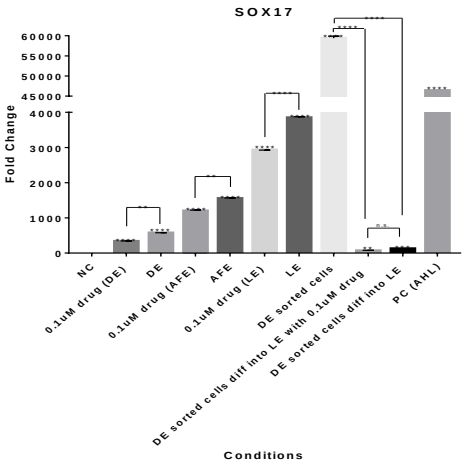
SOX17
Fold Change
Conditions
NC
0.1uM drug (DE)
DE
0.1uM drug (AFE)
AFE
0.1uM drug (LE)
LE
DE sorted cells
DE sorted cells diff into LE with 0.1uM drug
DE sorted cells diff into LE
PC (AHL)

M

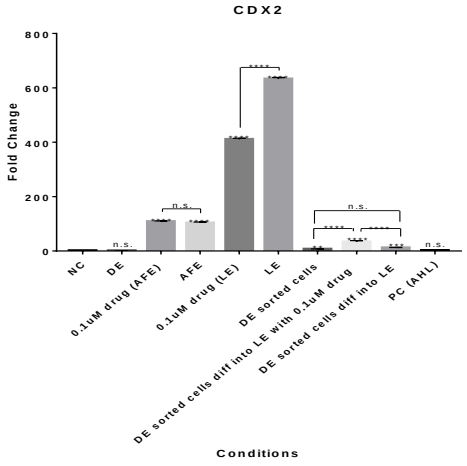
CDX2
Fold Change
Conditions
NC
DE
0.1uM drug (AFE)
AFE
0.1uM drug (LE)
LE
DE sorted cells
DE sorted cells diff into LE with 0.1uM drug
DE sorted cells diff into LE
PC (AHL)

N

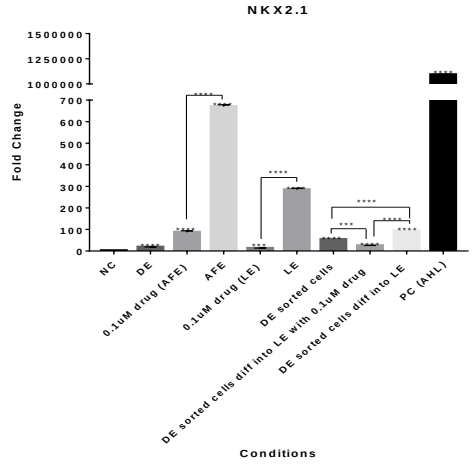
NKX2.1
Fold Change
Conditions
NC
DE
0.1uM drug (AFE)
AFE
0.1uM drug (LE)
LE
DE sorted cells
DE sorted cells diff into LE with 0.1uM drug
DE sorted cells diff into LE
PC (AHL)

O

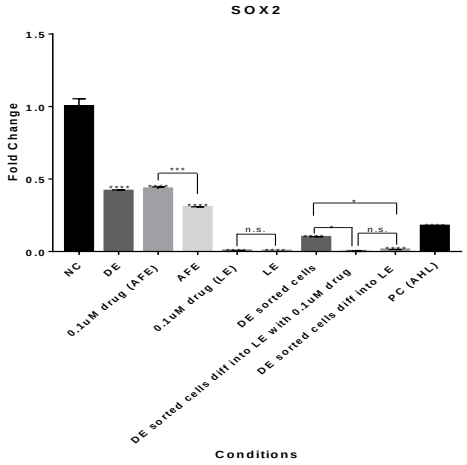
SOX2
Fold Change
Conditions
NC
DE
0.1uM drug (AFE)
AFE
0.1uM drug (LE)
LE
DE sorted cells
DE sorted cells diff into LE with 0.1uM drug
DE sorted cells diff into LE
PC (AHL)

Figure 10: Overall, cell viability decreased with each subsequent stage of differentiation. Cell morphology of undifferentiated vShiPS and vShiPS that were induced into definitive endoderm and subsequently into lung endoderm when exposed to the given culture conditions. All images are at 20x magnification.
Scale bar = 200um

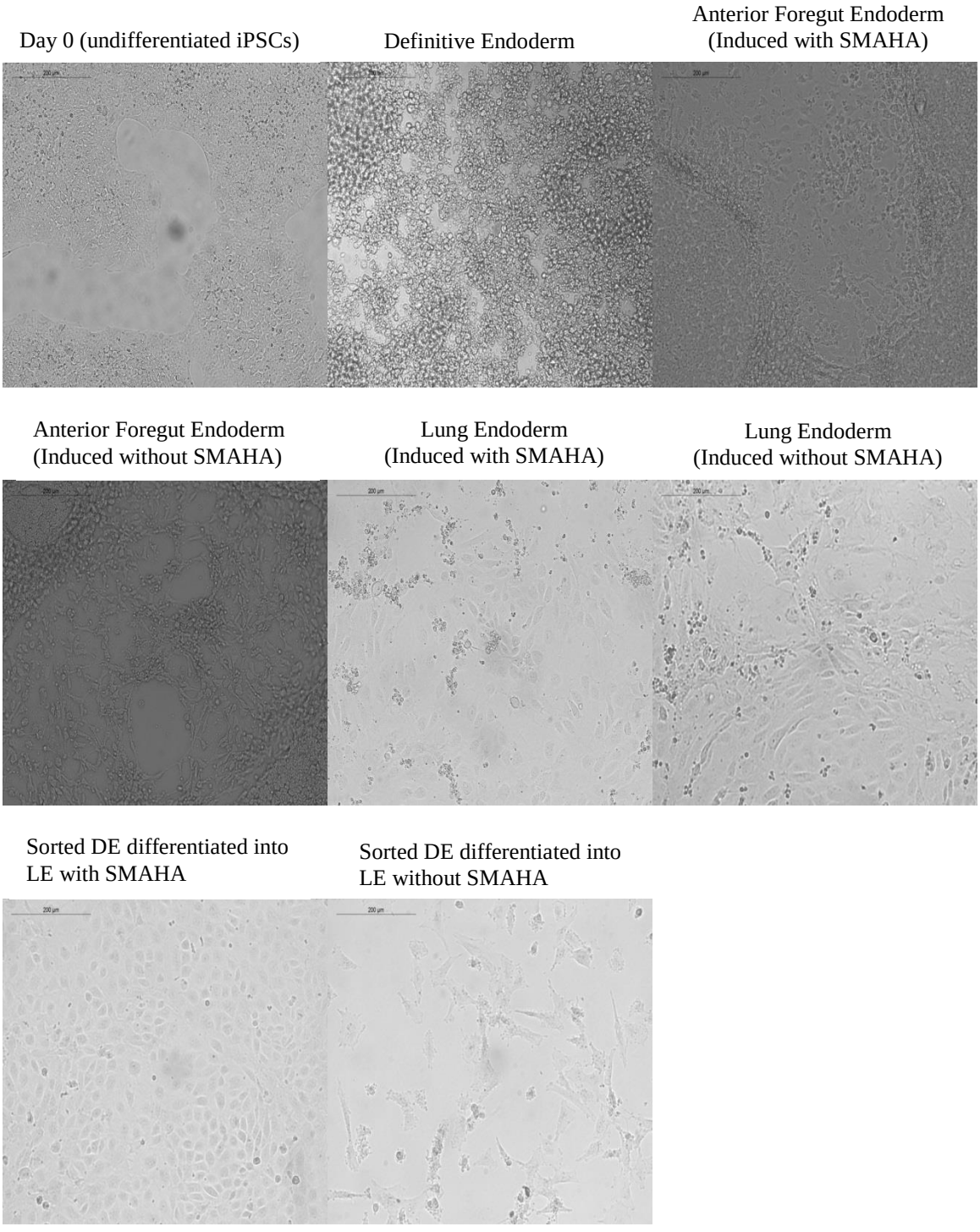

Tables

Table 1: Primary Antibody List

Antibody	Source
SOX2	R&D, goat polyclonal, AF2018
SOX9	R&D, goat polyclonal, AF3075
SOX17	R&D, goat polyclonal, AF1924
FOXA2	Santa Cruz Technology, goat polyclonal, sc-655
TUJ1	Sigma, mouse monoclonal, T8578
PAX8	Abcam, mouse monoclonal, ab53490
NKX2.1	Abcam, rabbit polyclonal, ab 76013
P63	Santa Cruz Technology, mouse monoclonal, sc-56188
CDX2	BioGenex, mouse monoclonal, CDX2-88

Table 2: Gene Expression Levels of the Three Cell Lines: Cells Cultured in SMAHA, Compared to No SMAHA

Cell Line	Day 4 (DE)	Day 8 (AFE)	Day 12 (LE)
L1	Pluripotency genes ↓ Endodermal genes ↓ Mesodermal genes ↑ Ectodermal genes ↑	NA	NA
Hiro	Pluripotency genes (no change) Endodermal genes ↑ Mesodermal genes ↑ Ectodermal genes ↑	NA	NA
vShiPS	Pluripotency genes ↑ Endodermal genes ↓ Mesodermal genes (no change) Ectodermal genes (no change)	Pluripotency genes ↓ Endodermal genes ↓ Mesodermal genes (no change) Ectodermal genes (no change)	Pluripotency genes ↓ Endodermal genes ↓ Mesodermal genes ↑ Ectodermal genes ↓

↓ = decrease
↑ = increase

References

Ahmad, S., Shlobin, O. A., & Nathan, S. D. (2011). Pulmonary Complications of Lung Transplantation. *Chest*, *139*(2), 402–411. http://doi.org/10.1378/chest.10-1048

American Lung Association. (2008). Lung Disease Data: 2008. *American Lung Association*, 41–54. Retrieved from http://www.lung.org/assets/documents/publications/lung-disease-data/LDD_2008.pdf

Bearzi, C., Rota, M., Hosoda, T., Tillmanns, J., Nascimbene, A., De Angelis, A., … Anversa, P. (2007). Human Cardiac Stem Cells. *Proceedings of the National Academy of Sciences*, *104*(35), 14068–14073. http://doi.org/10.1073/pnas.0706760104

Beltrami, A. P., Barlucchi, L., Torella, D., Baker, M., Limana, F., Chimenti, S., … Anversa, P. (2003). Adult Cardiac Stem Cells are Multipotent and Support Myocardial Regeneration. *Cell*, *114*(6), 763–776. http://doi.org/10.1016/S0092-8674(03)00687-1

Boffini, M., Ranieri, V. M., & Rinaldi, M. (2010). Lung Transplantation: Is It Still an Experimental Procedure? *Current Opinion in Critical Care*, *16*(1), 53–61. http://doi.org/10.1097/MCC.0b013e32833500a8

Botrugno, O. A., Santoro, F., & Minucci, S. (2009). Histone deacetylase inhibitors as a new weapon in the arsenal of differentiation therapies of cancer. *Cancer Letters*, *280*(2), 134–144. http://doi.org/10.1016/j.canlet.2009.02.027

Cao, L., Gibson, J. D., Miyamoto, S., Sail, V., Verma, R., Rosenberg, D. W., … Giardina, C. (2011). Intestinal Lineage Commitment of Embryonic Stem Cells. *Differentiation*, *81*(1), 1–10. http://doi.org/10.1016/j.diff.2010.09.182

Cedar, H., & Bergman, Y. (2009). Linking DNA Methylation and Histone Modification: Patterns and Paradigms. *Nature Reviews Genetics*, *10*(5), 295–304. http://doi.org/10.1038/nrg2540

Centers for Disease Control and Prevention. (2004). Annual Smoking-Attributable Mortality, Years of Potential Life Lost, and Productivity Losses - United States, 1997-2001. *Morbidity and Mortality Weekly Report*, *53*(8), 625–628.

Chang, S., Young, B. D., Li, S., Qi, X., Richardson, J. A., & Olson, E. N. (2006). Histone Deacetylase 7 Maintains Vascular Integrity by Repressing Matrix Metalloproteinase 10. *Cell*, *126*(2), 321–334. http://doi.org/10.1016/j.cell.2006.05.040

Chen, L., Wilson, D., Jayaram, H. N., & Pankiewicz, K. W. (2007). Dual Inhibitors of Inosine Monophosphate Dehydrogenase and Histone Deacetylases for Cancer Treatment. *Journal of Medicinal Chemistry*, *50*(26), 6685–6691. http://doi.org/10.1021/jm070864w

Evans, M. J., Cabral, L. J., Stephens, R. J., & Freeman, G. (1973). Renewal of Alveolar Epithelium in the Rat Following Exposure to NO2. *The American Journal of Pathology*, *70*(2), 175–98. Retrieved from http://www.pubmedcentral.nih.gov/articlerender.fcgi?artid=1903972&tool=pmcentrez&rendertype=abstract

Gilpin, S. E., Ren, X., Okamoto, T., Guyette, J. P., Mou, H., Rajagopal, J., … Ott, H. C.

(2014). Enhanced Lung Epithelial Specification of Human Induced Pluripotent Stem Cells on Decellularized Lung Matrix. *Annals of Thoracic Surgery*, *98*(5), 1721–1729. http://doi.org/10.1016/j.athoracsur.2014.05.080

Glozak, M. A., Sengupta, N., Zhang, X., & Seto, E. (2005). Acetylation and Deacetylation of Non-Histone Proteins. *Gene*, *363*(1-2), 15–23. http://doi.org/10.1016/j.gene.2005.09.010

Green, M. D., Chen, A., Nostro, M.-C., D'Souza, S. L., Schaniel, C., Lemischka, I. R., … Snoeck, H.-W. (2011). Generation of Anterior Foregut Endoderm from Human Embryonic and Induced Pluripotent Stem Cells. *Nature Biotechnology*, *29*(3), 267–272. http://doi.org/10.1038/nbt.1788

Herriges, M., & Morrisey, E. E. (2014). Lung Development: Orchestrating the Generation and Regeneration of a Complex Organ. *Development*, *141*(3), 502–513. http://doi.org/10.1242/dev.098186

Hirai, H., Firpo, M., & Kikyo, N. (2012). Establishment of LIF-dependent human iPS cells closely related to basic FGF-dependent authentic iPS cells. *PloS One*, *7*(6), e39022. http://doi.org/10.1371/journal.pone.0039022

Hirai, H., Katoku-Kikyo, N., Karian, P., Firpo, M., & Kikyo, N. (2012). Efficient iPS cell production with the myod transactivation domain in serum-free culture. *PLoS ONE*, *7*(3), 1–9. http://doi.org/10.1371/journal.pone.0034149

Ikonomou, L., & Kotton, D. N. (2015). Derivation of Endodermal Progenitors from Pluripotent Stem Cells. *Journal of Cellular Physiology*, *230*(2), 246–258. http://doi.org/10.1002/jcp.24771

Kajstura, J., Rota, M., Hall, S. R., Hosoda, T., D'Amario, D., Sanada, F., … Anversa, P. (2014). Evidence for Human Lung Stem Cells. *New England Journal of Medicine*, *364*(19), 1795–1806. http://doi.org/10.1056/NEJMoa1313731

Kim, H.-J., & Bae, S.-C. (2011). Histone Deacetylase Inhibitors: Molecular Mechanisms of Action and Clinical Trials as Anti-Cancer Drugs. *American Journal of Translational Research*, *3*(2), 166–179.

Kim, M.-S., Fielitz, J., McAnally, J., Shelton, J. M., Lemon, D. D., McKinsey, T. a, … Olson, E. N. (2008). Protein Kinase D1 Stimulates MEF2 Activity in Skeletal Muscle and Enhances Muscle Performance. *Molecular and Cellular Biology*, *28*(11), 3600–3609. http://doi.org/10.1128/MCB.00189-08

Knutson, S. K., Chyla, B. J., Amann, J. M., Bhaskara, S., Huppert, S. S., & Hiebert, S. W. (2008). Liver-Specific Deletion of Histone Deacetylase 3 Disrupts Metabolic Transcriptional Networks. *The EMBO Journal*, *27*(7), 1017–28. http://doi.org/10.1038/emboj.2008.51

Kretsovali, A., Hadjimichael, C., & Charmpilas, N. (2012). Histone Deacetylase Inhibitors in Cell Pluripotency, Differentiation, and Reprogramming. *Stem Cells International*, *2012*. http://doi.org/10.1155/2012/184154

Lai, M.-J., Huang, H.-L., Pan, S.-L., Liu, Y.-M., Peng, C.-Y., Lee, H.-Y., … Liou, J.-P. (2012). Synthesis and Biological Evaluation of 1-arylsulfonyl-5-(N-hydroxyacrylamide)indoles as Potent Histone Deacetylase Inhibitors with Antitumor Activity in Vivo. *Journal of Medicinal Chemistry*, *55*(8), 3777–91. http://doi.org/10.1021/jm300197a

Leeman, K. T., Fillmore, C. M., & Kim, C. F. (2014). *Lung Stem and Progenitor Cells in Tissue Homeostasis and Disease*. *Current Topics in Developmental Biology* (1st ed., Vol. 107). Elsevier Inc. http://doi.org/10.1016/B978-0-12-416022-4.00008-1

Li, B., Carey, M., & Workman, J. L. (2007). The Role of Chromatin during Transcription. *Cell*, *128*(4), 707–719. http://doi.org/10.1016/j.cell.2007.01.015

Li, E. (2002). Chromatin Modification and Epigenetic Reprogramming in Mammalian Development. *Nature Reviews Genetics*, *3*(9), 662–673. http://doi.org/10.1038/nrg887

Liu, Z., Tong, Y., Liu, Y., Liu, H., Li, C., Zhao, Y., & Zhang, Y. (2014). Effects of Suberoylanilide Hydroxamic Acid (SAHA) Combined with Paclitaxel (PTX) on Paclitaxel-Resistant Ovarian Cancer Cells and Insights into the Underlying Mechanisms. *Cancer Cell International*, *14*(1), 112. http://doi.org/10.1186/s12935-014-0112-x

Longmire, T. A., Ikonomou, L., Hawkins, F., Christodoulou, C., Cao, Y., Jean, J. C., … Kotton, D. N. (2012). Efficient Derivation of Purified Lung and Thyroid Progenitors from Embryonic Stem Cells. *Cell Stem Cell*, *10*(4), 398–411. http://doi.org/10.1016/j.stem.2012.01.019

Marks, P. a, & Breslow, R. (2007). Dimethyl Sulfoxide to Vorinostat: Development of this Histone Deacetylase Inhibitor as an Anticancer Drug. *Nature Biotechnology*, *25*(1), 84–90. http://doi.org/10.1038/nbt1272

Méjat, A., Ramond, F., Bassel-Duby, R., Khochbin, S., Olson, E. N., & Schaeffer, L. (2005). Histone Deacetylase 9 Couples Neuronal Activity to Muscle Chromatin Acetylation and Gene Expression. *Nature Neuroscience*, *8*(3), 313–321. http://doi.org/10.1038/nn1408

Miniño, A. M., Heron, M. P., Murphy, S. L., & Kochanek, K. D. (2007). Deaths: Final Data for 2004. *National Vital Statistics Reports*, *55*(19), 1–119.

Montgomery, R. L., Hsieh, J., Barbosa, A. C., Richardson, J. a, & Olson, E. N. (2009). Histone Deacetylases 1 and 2 Control the Progression of Neural Precursors to Neurons During Brain Development. *Proceedings of the National Academy of Sciences*, *106*(19), 7876–7881. http://doi.org/10.1073/pnas.0902750106

Montgomery, R. L., Potthoff, M. J., Haberland, M., Qi, X., Matsuzaki, S., Humphries, K. M., … Olson, E. N. (2008). Maintenance of Cardiac Energy Metabolism by Histone Deacetylase 3 in Mice. *Journal of Clinical Investigation*, *118*(11), 3588–3597. http://doi.org/10.1172/JCI35847

Mou, H., Zhao, R., Sherwood, R., Ahfeldt, T., Lapey, A., Wain, J., … Rajagopal, J. (2012a). Generation of multipotent lung and airway progenitors from mouse ESCs and patient-specific cystic fibrosis iPSCs. *Cell Stem Cell*, *10*(4), 385–397. http://doi.org/10.1016/j.stem.2012.01.018

Mou, H., Zhao, R., Sherwood, R., Ahfeldt, T., Lapey, A., Wain, J., … Rajagopal, J. (2012b). Generation of Multipotent Lung and Airway Progenitors from Mouse ESCs and Patient-Specific Cystic Fibrosis iPSCs. *Cell Stem Cell*, *10*(4), 385–397. http://doi.org/10.1016/j.stem.2012.01.018

NIH/NHLBI. (2012). Morbidity & Mortality: 2012 Chart Book on Cardiovascular, Lung, and Blood Diseases. *National Insitutes of Health/National Heart, Lung, and Blood*

Institute, 116. Retrieved from http://www.nhlbi.nih.gov/resources/docs/2012_ChartBook_508.pdf\nhttp://www.nhlbi.nih.gov/resources/docs/2012_ChartBook.pdf

Orlic, D., Fischer, R., Nishikawa, S., Nienhuis, a W., & Bodine, D. M. (1993). Purification and Characterization of Heterogeneous Pluripotent Hematopoietic Stem Cell Populations Expressing High Levels of c-kit Receptor. *Blood*, *82*(3), 762–70. Retrieved from http://www.ncbi.nlm.nih.gov/pubmed/7687891

Peake, J. L., Reynolds, S. D., Stripp, B. R., Stephens, K. E., & Pinkerton, K. E. (2000). Alteration of Pulmonary Neuroendocrine Cells during Epithelial Repair of Naphthalene-Induced Airway Injury. *The American Journal of Pathology*, *156*(1), 279–86. http://doi.org/10.1016/S0002-9440(10)64728-1

Schmeckebier, S., Mauritz, C., Katsirntaki, K., Sgodda, M., Puppe, V., Duerr, J., … Martin, U. (2013). Keratinocyte Growth Factor and Dexamethasone Plus Elevated cAMP Levels Synergistically Support Pluripotent Stem Cell Differentiation into Alveolar Epithelial Type II Cells. *Tissue Engineering*, *19*(7-8), 938–951. http://doi.org/10.1089/ten.TEA.2012.0066

Sherwood, R. I., Maehr, R., Mazzoni, E. O., & Melton, D. A. (2011). Wnt Signaling Specifies and Patterns Intestinal Endoderm. *Mechanisms of Development*, *128*(7-10), 387–400. http://doi.org/10.1016/j.mod.2011.07.005

Spence, J. R., Mayhew, C. N., Rankin, S. A., Kuhar, M. F., Vallance, J. E., Tolle, K., … Wells, J. M. (2010). Directed Differentiation of Human Pluripotent Stem Cells into Intestinal Tissue In Vitro. *Nature*, *470*(7332), 105–109. http://doi.org/10.1038/nature09691

Takahashi, K., Tanabe, K., Ohnuki, M., Narita, M., Ichisaka, T., Tomoda, K., & Yamanaka, S. (2007). Induction of Pluripotent Stem Cells from Adult Human Fibroblasts by Defined Factors. *Cell*, *131*(5), 861–872. http://doi.org/10.1016/j.cell.2007.11.019

Van Winkle, L. S., Buckpitt, a R., Nishio, S. J., Isaac, J. M., & Plopper, C. G. (1995). Cellular Response in Naphthalene-Induced Clara Cell Injury and Bronchiolar Epithelial Repair in Mice. *The American Journal of Physiology*, *269*(6), 800–818.

Vega, R. B., Matsuda, K., Oh, J., Barbosa, A. C., Yang, X., Meadows, E., … Olson, E. N. (2004). Histone Deacetylase 4 Controls Chondrocyte Hypertrophy during Skeletogenesis. *Cell*, *119*(4), 555–566. http://doi.org/10.1016/j.cell.2004.10.024

Wada, T., Kikuchi, J., Nishimura, N., Shimizu, R., Kitamura, T., & Furukawa, Y. (2009). Expression Levels of Histone Deacetylases Determine the Cell Fate of Hematopoietic Progenitors. *Journal of Biological Chemistry*, *284*(44), 30673–30683. http://doi.org/10.1074/jbc.M109.042242

Wang, Y., Tian, Y., Morley, M. P., Lu, M. M., DeMayo, F. J., Olson, E. N., & Morrisey, E. E. (2013). Development and Regeneration of Sox2+ Endoderm Progenitors are Regulated by a HDAC1/2-Bmp4/Rb1 Regulatory Pathway. *Developmental Cell*, *24*(4), 345–358. http://doi.org/10.1016/j.devcel.2013.01.012

Wilting, R. H., Yanover, E., Heideman, M. R., Jacobs, H., Horner, J., van der Torre, J., … Dannenberg, J.-H. (2010). Overlapping Functions of Hdac1 and Hdac2 in Cell Cycle Regulation and Haematopoiesis. *The EMBO Journal*, *29*(15), 2586–2597.

http://doi.org/10.1038/emboj.2010.136
Wong, A. P., Keating, A., Lu, W., Duchesneau, P., Wang, X., Sacher, A., … Waddell, T. K. (2009). Identification of a Bone Marrow-Derived Epithelial-Like Population Capable of Repopulating Injured Mouse Airway Epithelium. *Journal of Clinical Investigation*, *119*(2), 336–348. http://doi.org/10.1172/JCI36882DS1
Wong, A. P., & Rossant, J. (2013). Generation of Lung Epithelium from Pluripotent Stem Cells. *Current Pathobiology Reports*, *1*(2), 137–145. http://doi.org/10.1007/s40139-013-0016-9
Yang, B., Yu, D., Liu, J., Yang, K., Wu, G., & Liu, H. (2015). Antitumor Activity of SAHA, a Novel Histone Deacetylase Inhibitor, Against Murine B Cell Lymphoma A20 Cells in Vitro and in Vivo. *Tumour Biology: The Journal of the International Society for Oncodevelopmental Biology and Medicine*, *36*(7), 5051–61. http://doi.org/10.1007/s13277-015-3156-1
Yang, X.-J., & Seto, E. (2008). The Rpd3/Hda1 Family of Lysine Deacetylases: From Bacteria and Yeast to Mice and Men. *Nature Reviews Molecular Cell Biology*, *9*(3), 206–218. http://doi.org/10.1038/nrm2346
Ye, L., Muench, M. O., Fusaki, N., Beyer, A. I., Wang, J., Qi, Z., … Kan, Y. W. (2013). Blood cell-derived induced pluripotent stem cells free of reprogramming factors generated by Sendai viral vectors. *Stem Cells Translational Medicine*, *2*(8), 558–66. http://doi.org/10.5966/sctm.2013-0006
Yoshida, M., Matsuyama, A., Komatsu, Y., & Nishino, N. (2003). From Discovery to the Coming Generation of Histone Deacetylase Inhibitors. *Current Medicinal Chemistry*, *10*(22), 2351–2358. http://doi.org/10.2174/0929867033456602
Yusen, R. D. (2009). Technology and Outcomes Assessment in Lung Transplantation. *Proceedings of the American Thoracic Society*, *6*(1), 128–136. http://doi.org/10.1513/pats.200809-102GO
Yusen, R. D., Shearon, T. H., Qian, Y., Kotloff, R., Barr, M. L., Sweet, S., … Murray, S. (2010). Lung transplantation in the United States, 1999-2008. *American Journal of Transplantation*, *10*(4), 1047–1068. http://doi.org/10.1111/j.1600-6143.2010.03055.x